12-2013

Characterization of Complexes of 2,2-cis [Rh2(N{C6H5}COCH3)4] with Nitriles.

Megan Ketron
East Tennessee State University

Characterization of Complexes of 2,2-*cis* $[Rh_2(N\{C_6H_5\}COCH_3)_4]$ with Nitriles

Thesis Submitted in Partial Fulfillment of Honors-in-Discipline in Chemistry

By: Megan Ketron

The Honors College

Honors-in-Discipline Program

East Tennessee State University

November 10, 2013

_____

Dr. Cassandra Eagle, Faculty Mentor

_____

Dr. Peter Zhao, Faculty Reader

_____

Dr. Teresa Haynes, Faculty Reader

Table of Contents

List of Figures

List of Tables

Introduction

Dirhodium complexes have been known as efficient and effective catalysts for the synthesis of pyrethrins.[1,2] Pyrethrins are organic compounds that act as potent, low toxicity insecticides. The insecticide acts as a neurotoxin that attacks the nervous system of an insect. Once the nervous system of the insect is shut down, death immediately follows.[3] Pyrethrins are gradually replacing organophosphates and organochlorides, which are common ingredients in insecticides.[4] Pyrethrins effectively protect against human lice, mosquitoes, cock roaches, beetles, flies, and fleas.[5] An LD50 value is a measure of the acute toxicity of a substance that kills fifty percent of the test population.[6] With an LD50 of pyrethrins being 750 mg/kg for children and 1000 mg/kg for adults, small amounts of pyrethrins could be accidentally consumed without fatal poisoning.[5] Pyrethrins are naturally found in the seed case of a chrysanthemum flower. With the increasing demand for pyrethrin insecticides, synthesis of these compounds is necessary. The understanding of the catalyst that works best for their synthesis is also necessary.

Rhodium acetate, a complex discovered by Teyssie in 1973, is a rhodium(II) carboxylate that consists of two Rh(II) atoms and four bridging acetate ligands.[7] The core structure of all rhodium(II) complexes with four bridging ligands will be referred to as Rh_2L_4. Rhodium acetate can be synthesized from rhodium trichloride by the following general reaction shown in Figure 1.[8]

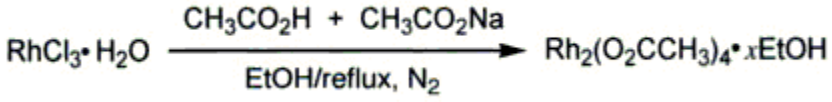

Figure 1. The reaction for the synthesis of rhodium acetate.

Rhodium acetate is a versatile catalyst and is soluble in a plethora of solvents such as water, ethanol, acetic acid, acetonitrile, and acetone.[9] This complex has a paddlewheel type structure

with each rhodium atom having square pyramidal coordination with an open coordination site. Figure 2 shows a rhodium(II) carboxylate that clearly distinguishes the axial and equatorial positions. The two rhodium atoms are bound to each other, and each rhodium atom has four equatorially bound oxygens and an available axial position that serves as the catalytic site. The Rh—Rh bond, with an average length of 2.35-2.45 Å, stabilizes the dimeric structure.[8] In a catalyzed reaction, a carbene binds to the catalytic site of a rhodium atom. Understanding electronic and structural properties of the metal carbene bond is of great importance. The bonding mode for a rhodium carbenoid is discussed in greater detail later in the introduction.

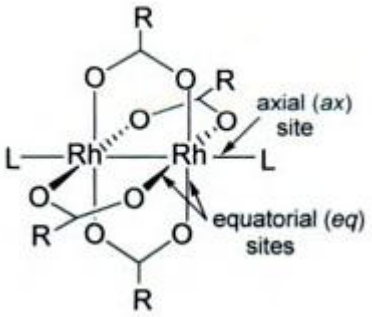

Figure 2. The structure of a rhodium (II) carboxylate.

The modification of the dirhodium core via ligand exchange can create a more selective catalyst.[8] The bridging acetate ligands can be exchanged to carboxamidates, amidinates, and thiocarboxylates to name a few. The structures of these common ligands are shown in Table 1.[8]

Table 1. Structures of common bridging ligands.

Ligand	Carboxylate	Carboxamidates	Amidinates	Thiocarboxylates
Structure	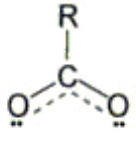 carboxylates	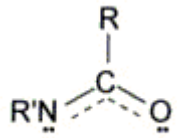 carboxamidates	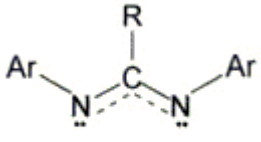 amidinates	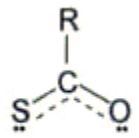 thiocarboxylates

The varying ligands change the electronic properties of the metal, which changes how the catalyst works. Carboxamidate ligands bound to a dirhodium catalyst are electron rich, which increases the electron density around the rhodium centers. Most of the research completed for this thesis involved the carboxamidate ligands where R is CH_3 and R' is C_6H_5. These specialty ligands are called N-phenylacetamidates.[8]

There are four possible geometric isomers of rhodium(II) carboxamidate complexes, which are shown in Figure 3. These include 2,2-cis, 2,2-trans, 3,1, and 4,0. The numbers correspond to the number of nitrogens connected to each rhodium atom.

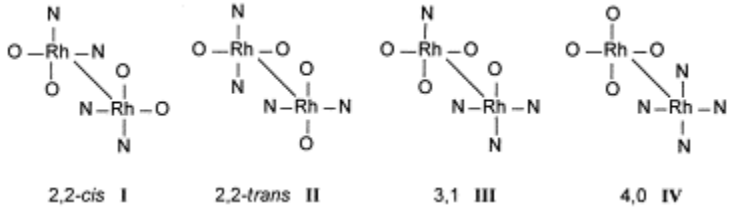

Figure 3. The geometric isomers of rhodium(II) carboxamidate complexes.

The 2,2-*trans* isomer has two nitrogens bound equatorially to each rhodium atom in the trans configuration. The point group of the immediate coordination sphere is D_{2h}.[8] The 2,2-*cis* isomer has two nitrogens bound equatorially to each rhodium atom in the cis configuration. The point group of the immediate coordination sphere is C_{2h}.[8] The 3,1 isomer has three nitrogens bound equatorially to one rhodium atom and only one bound to the other rhodium atom. The point group of the immediate coordination sphere is C_s.[8] The 4,0 isomer has four nitrogens bound equatorially to one rhodium atom and none bound to the other rhodium atom. The point group of the immediate coordination sphere is C_{4v}.[8] Each of these isomers have been successfully isolated and characterized by Doyle and/or Eagle. N-phenylacetamidates are the ligands used specifically for this research. These have a phenyl ring bound to each nitrogen atom and a

methyl group bound to the bridging carbon. The geometric isomer of interest is the 2,2-*cis* isomer. Figure 4 shows the structure of 2,2-*cis* $[Rh_2(N\{C_6H_5\}COCH_3)_4]$.

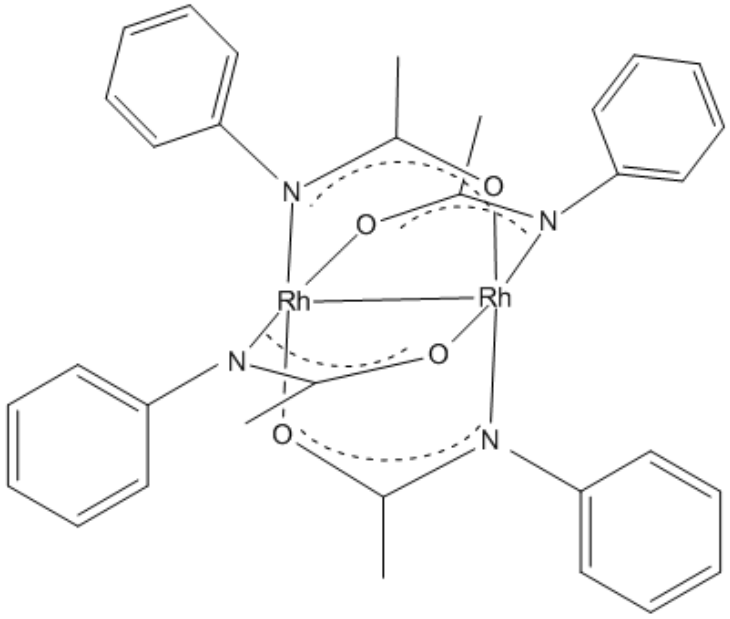

Figure 4. 2,2-*cis* $[Rh_2(N\{C_6H_5\}COCH_3)_4]$ with axial ligands omitted.

Experimental data from previously published similar dirhodium complexes provide good comparisons for bond lengths and angles. The complex 2,2-*cis*-$[Rh2(N\{C_6H_5\}COCH_3)_4]\cdot 2DMSO$ published by Bear et al. in 1987 has two rhodium atoms bound to one another with equatorial oxygens and nitrogens at ninety degree angles from one another.[10] They solved the crystal structure for a complex with dimethyl sulfoxide (DMSO) bound to both axial sites. The Rh—Rh bond length was 2.448(1) Å. The torsion angles (N—Rh—Rh—O) were found to be 13.1° for compound 1 and 3.48°. The torsion angles indicate how much the molecule is twisted from planarity. This is important because it indicates how available the catalytic site is. If the torsion angles are too high, there is less of a chance that something will bind to the catalytic site on the rhodium atom.

The complex 2,2-*trans*-$[Rh_2(N\{C_6H_5\}COCH_3)_4]\cdot 2NCC_6H_5$ was published by Eagle et al. in 2000.[11] It has a similar core structure to Bear's complex, but the nitrogens are positioned at 180° from one another in the *trans* configuration. The Rh—Rh bond distance was 2.422 Å. The torsion angles (N—Rh—Rh—O) of 9.03° and 11.89° are relatively larger than the Bear et al. complex. This complex is slightly twisted from the plane of the molecule and this is likely due to steric effects.[11] The axial Rh—N—C bond angles were 178.5(5)° and 169.3(5)°. These angles are of interest because the nitrile has a triple bond (N≡C), which means that the Rh—N—C bond should be linear.

Eagle et al. published the 2,2-*trans*-$Rh_2[N(C_9H_{11})COCH_3]_4\cdot 2NCC_6H_5$ complex in 2012.[12] Each phenyl ring has three methyl groups evenly spaced out. The Rh—Rh bond length was 2.429 Å. This is the most symmetric of each of the complexes as it is tetragonal with a space group of $P42_1c$. The axial Rh—N—C bond angle is perfectly linear because it is imposed by space group symmetry.[12]

Dirhodium catalysts bind with a carbene at the catalytic site in cyclopropanation reactions to form an intermediate known as a carbenoid. A carbene is a neutral divalent compound that acts as a strong electrophile.[13,14] A carbenoid is comprised of a metal atom bound to a carbene. The reactivity of a carbenoid can be altered by structural changes to the bridging ligands of the dirhodium catalyst, which results in more selective catalysts.[15] The rhodium carbenoid is hard to isolate and characterize directly because of the short life of carbenes. A model for the metal-carbene bond is desired in order to understand electronic and structural properties of the catalyst. Nitriles serve as effective models when bound at the axial site because they have similar bonding capabilities.

Extensive research has been completed on the rhodium carbene bond. It is known that a metal-carbene bond uses both σ-bonding and π-backbonding.[16] Both types of bonding mechanisms are shown in Figure 5.[17]

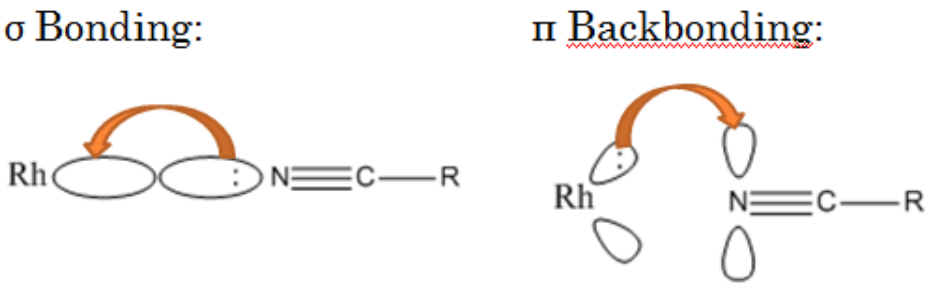

Figure 5. Representation of σ-bonding and π-backbonding.

The combination of both bonding modes creates a very stable but short lived bond.[18] A stable bond is formed when the energy of two atoms joined together is lower than the energy of the separate atoms.[19] σ-bonding occurs when the ligand acts as a lewis base and donates an electron pair to the metal. π-backbonding occurs when the metal acts as a lewis base and donates an electron pair to the ligand. Studying this bond presents a challenge because of the transient quality of carbenes, so a model of the bond is easier to study. Nitriles have similar bonding properties to carbenes because they are strong field ligands that are capable of σ-bonding and π-backbonding.[18] Nitriles have filled σ orbitals that can donate electrons to the metal and empty π* orbitals that are capable of accepting electrons donated from the metal atom. Nitriles provide a suitable bonding model for Rh_2L_4 complexes.

X-ray crystallography is a technique used to characterize compounds by determining the crystal structure. The spatial arrangement of atoms in a molecule is of interest to many scientists. In order to determine a crystal structure by X-ray diffraction, a high energy type of electromagnetic radiation must be used with very small wavelengths, similar to the size of atoms.

X-rays have wavelengths between 0.01 and 10 nm, and they work very well for penetrating microscopic objects. Single crystal x-ray diffraction was a main characterization technique of this thesis. A crystal is struck by a beam of x-rays and they diffract off of the atoms in a molecule and display a diffraction pattern. The diffraction pattern is captured by a CCD, which sends the data to software system on a computer. Diffraction patterns are unique for each molecule which allows for structure determination. The diffraction patterns, which are spatial arrangements of many unique reflections, show up as "spots" that account for individual atoms.[20] A three dimensional electron density map was formulated, and the computer software helped with solving the crystal structure. Bond lengths, bond angles, unit cell dimensions, disorder, etc. were all useful bits of information that can be obtained from a crystal structure. The crystal structure can be solved by using a variety of ways including direct methods and the Patterson method.

A crystal is a solid structure that consists of atoms positioned in an orderly arrangement. The atoms are packed together as efficiently as possible with repeating patterns. A unit cell is the smallest repeating, three dimensional pattern in a crystal lattice. A unit cell is usually described as a rectangular prism with side lengths described as a, b, and c, and the angles between them described as α, β, and γ. All useful information about a crystal structure can be obtained by using the unit cell since the rest of the crystal lattice consists of the same repeating pattern. There are seven existing crystal systems, and every crystal is categorized into one of the systems. They describe the symmetry of the crystal.

A diffractometer is used to generate the x-rays, isolate the appropriate wavelengths, direct the x-rays to the crystal, and collect the diffraction patterns. The crystal is mounted on a mounting pin which is attached to the goniometer. The goniometer rotates on three different

axes so it is able to collect diffraction patterns from all different angles. The x-rays are generated from a source of radiation. The diffractometer used in the Eagle research group has a molybdenum κ_α source. The Mo is bombarded with electrons at a high voltage, and characteristic x-rays are produced. Each atom in the periodic table has a characteristic wavelength, and Mo has a wavelength of 0.7107 Å.[21] The x-ray forms as a result of the electronic transitions that occur within an atom. One of the electrons is removed from the inner most shell of electrons, and an electron from an outer shell jumps to the inner shell. This transition of electrons causes an x-ray to form that has a unique wavelength related to the atom used in the source.[22]

The X-rays are focused using a monochromator. This allows the X-rays to be concentrated to a specific wavelength. The purpose of this is to create constructive interference between the many random X-rays so they will be in phase with one another. Constructive interference occurs when the rises and troughs of waves occur in sequence at the same place. The X-rays strike the crystal and they can diffract, transmit through the crystal, or reflect off the surface.[20] A beam stop is used to block any transmitted X-rays from reaching the detector. Reflected X-rays do not reach the detector, so only the diffracted X-rays are detected and analyzed. A diffraction pattern is able to be obtained by measuring the intensity of the scattered X-rays as a function of the angle.

The compound $[Rh_2(N\{C_6H_5\}COCH_3)_4]$ was synthesized with each of the following ligands in the axial position: benzonitrile, ortho-tolunitrile, and meta-tolunitrile. Each compound was crystallized and characterized using X-ray crystallography, FTIR, and NMR. Implications involving the rhodium-rhodium bond, the angle of the attached nitrile (Rh—N—C), and the bond at the axial site were studied and discussed. Changes in the crystal structures

occurring because of the different attached nitriles were observed. The bonding mode at the catalytic site was discovered for each molecule.

Methods and Materials

I. Materials:

1. Solvents
    a. Methanol
        - Used as supplied by Fischer Scientific
    b. Ethanol
        - Used as supplied by Fischer Scientific
    c. Acetonitrile
        - Used as supplied
    d. Ethyl Alcohol
        - Used as supplied
    e. Water
        - Used as supplied
    f. Acetone
        - Used as supplied
    g. Dichloromethane
        - Used as supplied
    h. Hexane
        - Used as supplied
    i. Toluene
        - Used over magnesium sulfate
2. Nitriles
    a. Benzonitrile

- Used as supplied

b. Ortho-tolunitrile

- Used as supplied

c. Meta-tolunitrile

- Used as supplied

3. Reagents

a. Rhodium trichloride trihydrate

- Supplied from Johnson Matthey Company as part of their precious metals loan program.
- Used as supplied

b. Sodium Acetate

- Used as supplied

c. Glacial Acetic Acid

- Used as supplied

II. Methods:

1. Synthesis of $Rh_2(O_2CCH_3)_4$
2. Synthesis of $[Rh_2(N\{C_6H_5\}COCH_3)_4]$• nitriles
3. Crystallization of $[Rh_2(N\{C_6H_5\}COCH_3)_4]$• nitriles
4. X-ray Crystallography
    a. A Rigaku XtaLAB mini bench top X-ray diffractometer was used.
5. Data Collection
6. Solving A Structure
7. IR Spectroscopy

a. A Shimadzu IR Prestige-21 spectrometer was used.

8. ^{1}H NMR Spectroscopy

    a. A JEOL NMR Spectrometer was used.

The Synthesis of Rhodium Acetate

Rhodium acetate was synthesized to use as a reagent in the synthesis of rhodium phenyl acetamide. A reflux apparatus was assembled with a column condenser, round bottom flask, reflux, stir bar, nitrogen adapter, stirring hot plate, and a heating mantle. The N_2 flowed in to the reflux apparatus on top of the column condenser and back out on top with the use of needles and a rubber septum cap, and the N_2 out line was connected to a mineral oil bubbler. The H_2O flowed in the column condenser on the bottom side and flowed out on the top side to a cup sink.

10 g of sodium acetate trihydrate, 100 ml of glacial acetic acid, and 100 ml of absolute ethanol were mixed in a round bottom flask. 4.972 g of rhodium trichloride trihydrate was added to the solution, and it turned a dark reddish color. To ready this solution for the reflux reaction, the stirring hot plate was set to about 400 rpm, the heating mantle was plugged into the 120 V variac (which was set at 60%), and the N_2 and H_2O were turned on. The solution was heated at reflux for 55 min. After 20 min, a green hue appeared in the solution. The amount of N_2 used was slightly increased at the beginning and end of the reflux reaction.

The solution was cooled and then filtered with a Buchner funnel and dried on the filtration apparatus under a water aspirator for one hour. The solid collected was a deep green color. The solid was mixed with 600 ml of boiling methanol. The boiling methanol solution was filtered, and the solid was dried and weighed as part of the recovery. The filtrate was reduced to about 400 ml and refrigerated overnight. The refrigerated solution was filtered the next day, then

the resulting solid boiled with methanol, and filtered again as before. The solid was dried and weighed as the second part of the recovery. This process was repeated a third time to yield a third and final recovery. This repetition was used in an attempt to recover as much product as possible. Each of the three samples produced were placed in a vacuum oven at 45 °C for 20 hours to remove methanol in the axial site. The percent yield was determined by using the combined weight of the three samples, and it was found to be 76.24%.

Synthesis of 2,2-*cis* $[Rh_2(N\{C_6H_5\}COCH_3)_4]$

The synthesis of 2,2-*cis* $Rh_2[N(C_6H_5)COCH_3]_4$ was completed by members of the Eagle research group.[23] This was done by using rhodium acetate.

Synthesis of 2,2-*cis* $[Rh_2(N\{C_6H_5\}COCH_3)_4]$• nitriles

Benzonitrile adduct of 2,2-*cis* $[Rh_2(N\{C_6H_5\}COCH_3)_4]$

Benzonitrile was attached as the axial ligand to each rhodium atom by the following experimental procedure. 0.010 g of 2,2-*cis* $[Rh_2(N\{C_6H_5\}COCH_3)_4]$ was weighed out and placed in a 6 dram vial. 18 mL of dichloromethane was added to the vial. This made a Kelly green colored solution. Next, 10 μL of benzonitrile was added via a gas-tight syringe. The solution immediately turned a light blue color. A small amount of acetone (2 μL) was added to the solution. The solution was transferred equally into 1 dram vials in preparation of crystal growth.

Ortho-tolunitrile adduct of 2,2-*cis* $[Rh_2(N\{C_6H_5\}COCH_3)_4]$

Ortho-tolunitrile was attached as the axial ligand to each rhodium atom by the following experimental procedure. 0.010 g of 2,2-*cis* $[Rh_2(N\{C_6H_5\}COCH_3)_4]$ was weighed out and

placed in a 6 dram vial. Next, 18 mL of dichloromethane was mixed in the vial, and a green solution was formed. Using a gas-tight syringe, 319.5 μL of ortho-tolunitrile and 2 μL of acetone were added to the solution. The solution turned a light bluish-green color. The solution was transferred, similar to the benzonitrile procedure above, into 1 dram vials in preparation of crystal growth.

Meta-tolunitrile adduct of 2,2-*cis* $[Rh_2(N\{C_6H_5\}COCH_3)_4]$

200 equivalents of meta-tolunitrile were used to achieve a crystal structure with two meta-tolunitriles; one attached to each rhodium atom. 0.010 g of 2,2-*cis* $[Rh_2(N\{C_6H_5\}COCH_3)_4]$ was placed in a 6 dram vial, and 18 mL of dichloromethane was added. The mixture produced a Kelly green solution. 319.5 μL of meta-tolunitrile was added via a gas-tight syringe, and the solution turned a light blue color. 2 μL of acetone was added, and no color change occurred as before. The solution was transferred equally into five 1 dram vials in preparation of crystal growth.

Crystallization Process of 2,2-*cis* $[Rh_2(N\{C_6H_5\}COCH_3)_4]$• nitriles

Benzonitrile adduct of 2,2-*cis* $[Rh_2(N\{C_6H_5\}COCH_3)_4]$

The solution with $[Rh_2(N\{C_6H_5\}COCH_3)_4]$• $2NCC_6H_5$ was transferred in equal amounts to seven 1 dram vials. The method of crystallization used was vapor diffusion. This process involved placing a small vial (1 dram) containing the solution and dichloromethane inside a large vial (6 dram) that held a solvent. The vapors diffused resulted in the formation of X-ray quality crystals in some cases. Seven different solvents were used in an attempt to crystallize $[Rh_2(N\{C_6H_5\}COCH_3)_4]$• $2NCC_6H_5$ in this experiment. They included: ethyl alcohol, ethanol, methanol, toluene, acetone, hexane, and water. The small vials were placed inside the large vials

and capped tightly. They were left alone to induce crystal growth. Crystals grew after about a week.

Ortho-tolunitrile adduct of 2,2-*cis* $[Rh_2(N\{C_6H_5\}COCH_3)_4]$

The solution of 2,2-*cis* $[Rh_2(N\{C_6H_5\}COCH_3)_4]$•$2NC\{2\text{-}CH_3\}C_6H_4$ was in seven 1 dram vials. The same seven solvents were used for crystal growth via vapor diffusion. The same procedure was used as the benzonitrile procedure above.

Meta-tolunitrile adduct of 2,2-*cis* $[Rh_2(N\{C_6H_5\}COCH_3)_4]$

The method of crystallization for meta-tolunitrile adduct was similar as it also used the method of vapor diffusion. The solution of 2,2-*cis* $[Rh_2(N\{C_6H_5\}COCH_3)_4]$•$2NC\{3\text{-}CH_3\}C_6H_4$ was in five 1 dram vials. Five different solvents were chosen to use for vapor diffusion. The chosen solvents were as follows: acetone, ethyl alcohol, methanol, hexane, and water. The solvents were placed inside five 6 dram vials at equal volumes of about 5 mL. The small vials containing the solution of 2,2-*cis* $[Rh_2(N\{C_6H_5\}COCH_3)_4]$•$2NC\{3\text{-}CH_3\}C_6H_4$ were placed inside the large vials with the various solvents. The large vials were capped and set aside for the duration of a week to allow crystallization.

X-ray Crystallography

A Rigaku XtaLAB mini bench top X-ray crystallography diffractometer was used to analyze single crystals. This model was manufactured in 2011. The diffractometer consists of a goniometer, an x-ray pattern board, a video camera to assist with mounting crystals, a low temperature apparatus, and software to analyze the data. All crystals are mounted on the tip of a mitogen loop. Stop cock grease was used to coax a chosen crystal from the site of growth to a

microscope slide for further analysis. All crystals to be mounted in the diffractometer were within 0.1 mm and 1 mm in size. If necessary, the crystal was cut to fit these parameters. STP was used to transfer the ready crystal from the microscope slide onto the tip of the mitogen loop.

The mitogen loop connected to the goniometer in the diffractometer by a strong magnet, and it was carefully placed on there so as not to jar the crystal off of the loop. The crystal was adjusted so the x-rays penetrate it right in the middle from all dimensions. The phi axis was unlocked so the other axes could be adjusted accordingly. The RAXVIDEO camera was used to guide this adjustment. The crystal was rotated along the phi axis, and moved slightly left or right and up or down from each angle to get it lined up in the center of the crosshairs. Once the crystal was accurately centered in the diffractometer, the data collection process began.

Data Collection

Crystal Clear software was used to collect the crystallographic data from the Rigaku XtaLabMini diffractometer. The process began with the collection of twelve initial images. These initial images were collected at random angles to get an overall simplified picture of the crystal. An initial unit cell was determined, and the crystal was given a space group. This allows one to determine if the crystal being analyzed was of good enough quality to collect a full data set. The initial images should have clear, distinct spots not in any noticeable arrangement. If the spots were lined up right beside each other, this indicates that there were multiple crystals grown on top of each other. The computer software matched up the spots with where the spots were calculated to be using the assigned space group. This was called integrating reflections, and the spots should mostly match up with the calculated spot positions.

When a full data set was collected, the crystal was rotated in all directions and bombarded with X-rays to get the full electron density map. About one thousand images were collected, reflections were integrated, structure factors were calculated, and a structure could potentially be solved. The crystal should fit into one of the seven crystal systems based on the symmetry of the atoms arranged in the crystal. If everything fit the model, the data from Crystal Clear is transferred to Crystal Structure for the structure solution process.

Solving A Structure

Crystal Structure was a software program used to take crystallographic data and solve a crystal structure. The space group the fits best with the data was suggested, but one can change it to see if other space groups work better. The technique used to solve a structure was trial and error. There were direct methods and Patterson methods that were used to match up data with known structures. Some common direct methods used were SIR92 and SIR2004. These methods seem to work the best. These methods provided the basic framework of the crystal structure.

Bond angles, bond distances, and symmetry related atoms helped with solving a structure with using knowledge about the molecule. Peaks of electron density arose, and the specific atoms they correspond to were decided. Thermal parameters were used to distinguish between the atoms. The input file showed the thermal parameters, and heavier atoms had larger thermal parameters while lighter atoms had smaller thermal parameters. The atoms were analyzed isotropically at first, which assumes the atoms are fixed in space. Atoms actually vibrate and move around realistically, so the atoms were eventually analyzed anisotropically to take the movements into consideration. Outliers are reflections that do not fit the model very well, which

could be because of a less than perfectly formed crystal lattice. A few of these outliers were removed to help achieve a better residual value (R value).

The R value measured how well the data fit the model. It used the calculated structure factors and the observed structure factors to determine a value using the equation below.

$$R\ value = \frac{\sum||F_{obs}| - |F_{calc}||}{\sum |F_{obs}|}$$

F_{obs} corresponds to observed structure factors, and F_{calc} corresponds to calculated structure factors. An acceptable R value was lower than five percent. Refinement was performed where a least squares program runs to tell you the residual value, weighted residual value, goodness of fit, and maximum shift over error. This information told how much the actual crystal structure varied from the calculated crystal structure.

IR Spectroscopy

A Shimadzu IR Prestige-21 spectrometer was used to collect all the IR data. An infrared spectrum was collected on each molecule to confirm the crystal structure. The peak of interest in an IR spectrum is the nitrile peak, which usually has an absorption peak around 2260-2220 cm^{-1}. The position of the nitrile peak provided some insight as to the type of bonding involved between the metal and the axial ligand. About 0.1 g of each adduct and isolated nitrile was individually placed on the eye of the FTIR for analysis.

^{1}H NMR

A JEOL NMR instrument operating at 400 MHz was used for NMR spectroscopic analysis. The proton NMR spectrum was taken on each molecule to evaluate the protons and

confirm the crystal structure. About 0.05 g of each adduct of 2,2-cis $Rh_2(N(C_6H_5)COCH_3)_4$ was dissolved in about 1 mL of dichloromethane and placed in an NMR tube. About 1 mL of d-chloroform was added. 32 scans were collected and analyzed.

Results and Discussion

1. ^{1}H NMR Data

The proton NMR spectrum was obtained for each of the following compounds: 2,2-cis $[Rh_2(N\{C_6H_5\}COCH_3)_4]$ uncomplexed, 2,2-*cis* $[Rh_2(N\{C_6H_5\}COCH_3)_4]$•benzonitrile, 2,2-*cis* $[Rh_2(N\{C_6H_5\}COCH_3)_4]$•ortho-tolunitrile, 2,2-*cis* $[Rh_2(N\{C_6H_5\}COCH_3)_4]$•meta-tolunitrile, and each of nitriles isolated. Comparisons were made about the chemical shifts of the protons in order to gain an understanding of the effect of bonding the nitriles to the dirhodium phenyl acetamide complex. Protons farther to the right side of the spectrum are at a lower energy and are considered to be shielded. Shielding refers to the electrons in a molecule shielding the nucleus. Protons on the left side of the spectrum are at a higher energy and are considered to be deshielded.

The ^{1}H NMR spectrum for the uncomplexed dirhodium phenyl acetamide complex is shown in Figure 6. The peaks of interest are described in Table 2 below.

Table 2. Proton NMR Peaks of interest for $[Rh_2(N\{C_6H_5\}COCH_3)_4]$

Peak	Chemical Shift (ppm)	Multiplicity	Interpretation
A	7.51	Doublet	Solvent Impurity
B	7.37	Triplet	Solvent Impurity
C	7.24	Triplet	N-Phenyl protons (ortho)
D	7.15	Triplet	N-Phenyl protons (para)
E	6.92	Doublet	N-Phenyl protons (meta)
F	3.49	Triplet	Solvent Impurity
G	2.18	Singlet	Solvent Impurity
H	1.91	Singlet	Methyl group
I	1.62	Singlet	Solvent Impurity
J	1.29	Doublet	Solvent Impurity

Peaks were expected to show for the protons on the phenyl rings attached to each nitrogen of the bridging ligands of the compound. The chemical shifts for both protons in the ortho position were represented by peak C. The meta position protons were peak E, and the para position proton was peak D. The nitrogen that the phenyl rings were attached to acted as an electron withdrawing group. The ortho and para protons were the most deshielded because of delocalization of the N—C—O group. The protons ortho to the nitrogen experienced the most deshielding because they had the closest proximity to the nitrogen, and had a chemical shift of 7.24 ppm. This peak showed up as a doublet because of one neighboring proton. The proton that was para to the nitrogen was the next most shielded with a chemical shift of 7.15 ppm. This proton neighbored two hydrogens, so it was a triplet. The protons meta to the nitrogen experienced the least shielding and had a chemical shift of 6.92 ppm. It made sense the peak was a triplet because of the two adjacent protons. The methyl group protons are represented by a singlet peak at 1.91 ppm. The peaks A, B, F, G, I, and J were all solvent impurities that came from the synthesis of $[Rh_2(N\{C_6H_5\}COCH_3)_4]$.

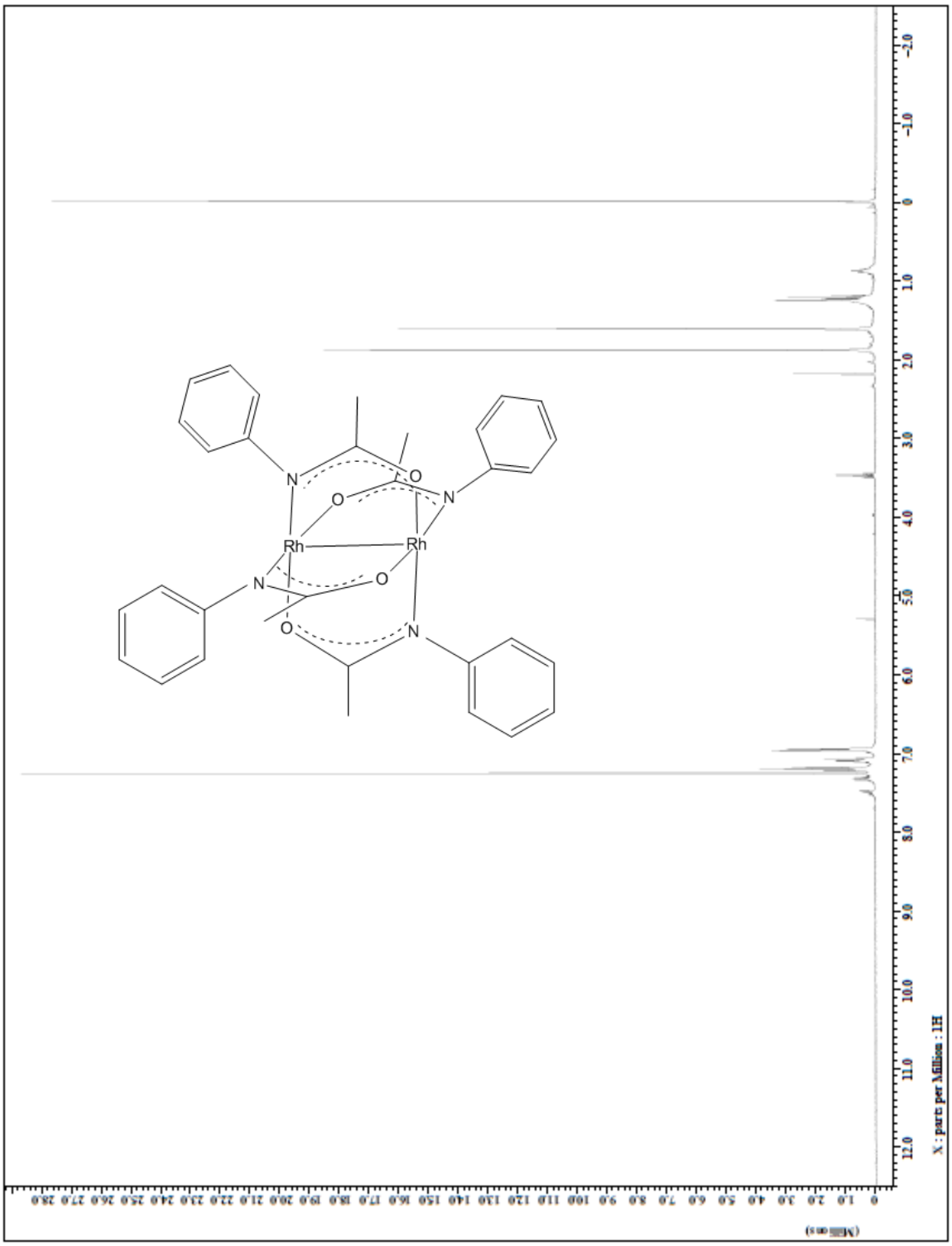

Figure 6. ^{1}H NMR Spectrum of uncomplexed 2,2-*cis* $[Rh_2(N\{C_6H_5\}COCH_3)_4]$

Figures 7 and 8 show the ^{1}H NMR spectrum for $[Rh_2(N\{C_6H_5\}COCH_3)_4]\cdot$benzonitrile and benzonitrile. Table 3 shows the NMR data for $[Rh_2(N\{C_6H_5\}COCH_3)_4]\cdot$benzonitrile and Table 4 shows for benzonitrile.

Table 3. The ^{1}H NMR data for $[Rh_2(N\{C_6H_5\}COCH_3)_4]\cdot$benzonitrile.

Peak	Chemical Shift (ppm)	Multiplicity	Interpretation
A	7.57	Multiplet	Nitrile proton
B	7.20	Triplet	Nitrile proton
C	7.12	Triplet	N-phenyl proton (meta)
D	6.98	Triplet	N-phenyl proton (para)
E	6.97	Doublet	N-phenyl proton (ortho)
F	3.49	Triplet	Solvent impurity
G	2.21	Doublet	Solvent impurity
H	1.90	Doublet	Solvent impurity
I	1.66	Doublet	Solvent impurity
J	1.25	Doublet	Solvent impurity
K	0.87	Singlet	Methyl group proton

Table 4. The ^{1}H NMR data for benzonitrile.

Peak	Chemical Shift (ppm)	Multiplicity	Interpretation
A	7.69	Triplet	Nitrile proton (ortho)
B	7.53	Triplet	Nitrile proton (para)
C	7.31	Doublet	Nitrile proton (meta)
D	1.61	Singlet	Solvent impurity

The axial ligand, benzonitrile, consists of a benzene ring with a nitrile (C≡N) attached. The nitrile acts as an electron withdrawing group, so the protons are more deshielded. When the benzonitrile is attached to the rhodium atom in the $[Rh_2(N\{C_6H_5\}COCH_3)_4]\cdot$benzonitrile complex, it caused the nitrile to act more as an electron donating group. This caused the nitrile protons to appear slightly more shielded for this complex. For isolated benzonitrile, peaks A, B, and C represent protons in the meta, para, and ortho positions respectively. The ortho position

protons were the most deshielded (7.69 ppm) because they were the closest to the C≡N functional group. This was a doublet because there was one adjacent hydrogen. The meta position was the least deshielded and had a triplet peak. The para position was also a triplet peak. The peak located at 1.69 ppm showed up because of a solvent impurity.

The $[Rh_2(N\{C_6H_5\}COCH_3)_4]$·benzonitrile complex had peaks in the ^1H NMR spectrum representing the nitrile phenyl protons, the N-phenyl protons, and the methyl group protons on the bridging acetamide ligands. Peaks A and B are for the N-phenyl protons. There are three distinct protons that have different chemical environments, but the peaks were so close together that they appeared as only two. These protons are the most deshielded because the nitogen as part of the bridging phenyl acetamide ligands acts as an electron withdrawing group. Peaks C, D, and E represent the nitrile phenyl protons. Peak C is the meta position protons and is a triplet, peak D is the para position proton and is also a triplet, and peak E is the ortho position protons and is a doublet. The protons that were ortho to the nitrogen are the most shielded because they were the closest. These protons are the most shielded because the Rh—N≡C bond acted as an electron donating group. There were many solvent impurity peaks (F, G, H, I, and J) in the range of 3.5-0.8 ppm. Peak K (0.87 ppm) represents the methyl group protons on the bridging ligands. This peak was a singlet because there were no adjacent protons.

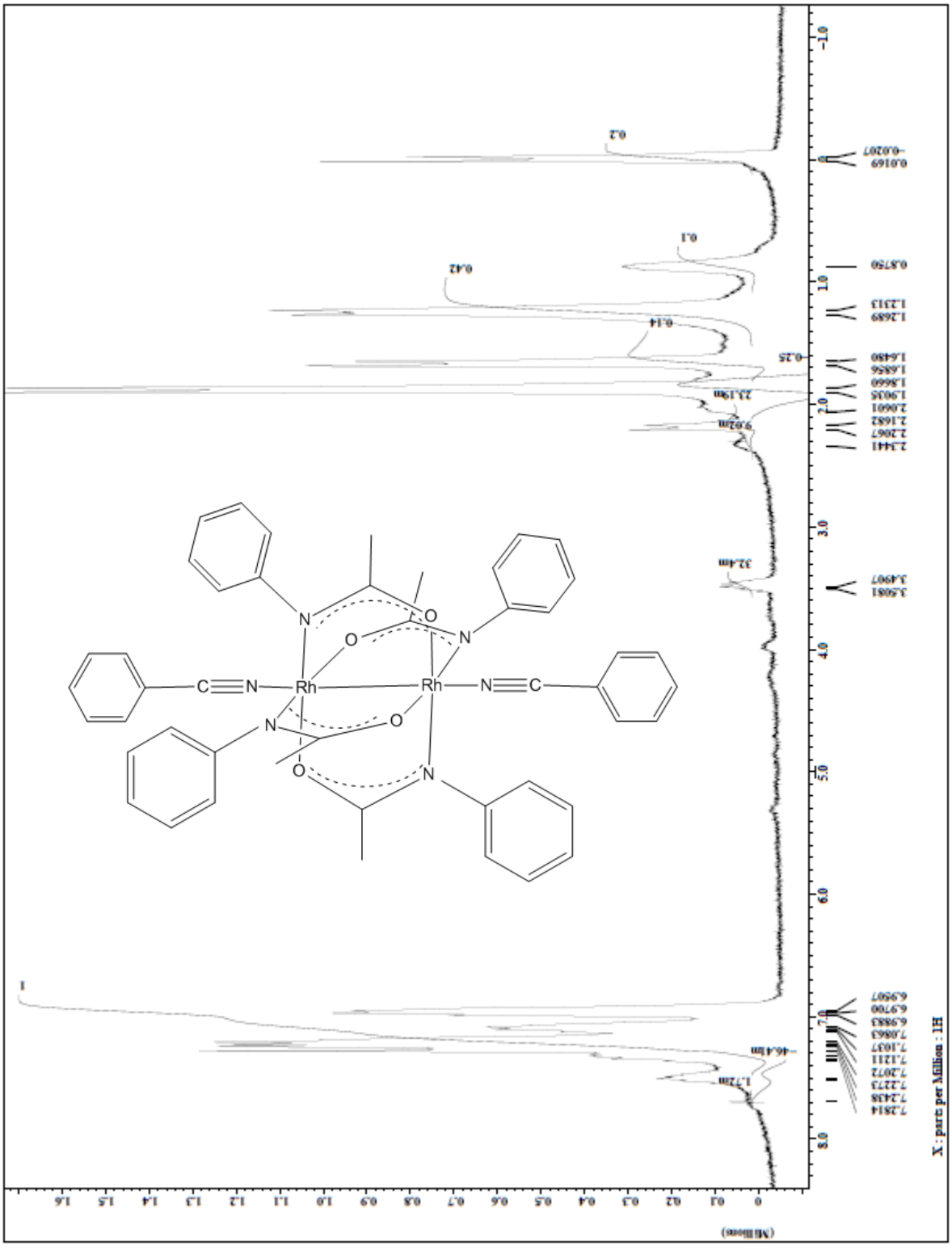

Figure 7. NMR spectrum of 2,2-*cis* $[Rh_2(N\{C_6H_5\}COCH_3)_4]\bullet 2NCC_6H_5$

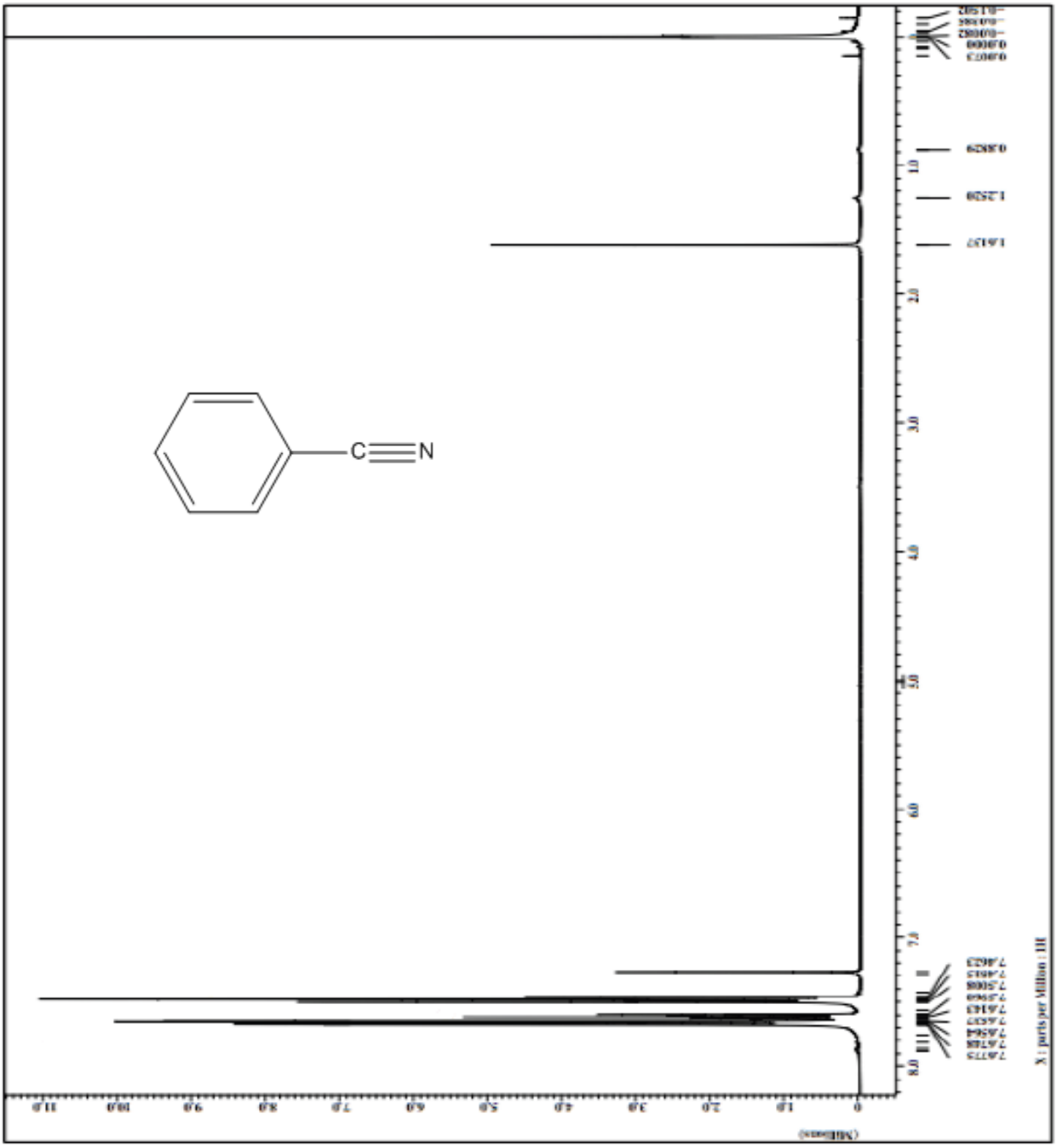

Figure 8. NMR Spectrum of benzonitrile.

The proton NMR spectrum for $[Rh_2(N\{C_6H_5\}COCH_3)_4]$·ortho-tolunitrile is shown in Figure 9. The spectrum for ortho-tolunitrile is shown in Figure 10. Table 5 shows all the peaks for $[Rh_2(N\{C_6H_5\}COCH_3)_4]$·ortho-tolunitrile, and Table 6 shows all the peaks for isolated ortho-tolunitrile.

Table 5. ^1H NMR data for $[Rh_2(N\{C_6H_5\}COCH_3)_4]$·ortho-tolunitrile.

Peak	Chemical Shift (ppm)	Multiplicity	Interpretation
A	7.48	Doublet	N-phenyl protons
B	7.27	Triplet	N-phenyl protons
C	7.19	Triplet	Nitrile phenyl protons
D	6.97	Triplet	Nitrile phenyl protons
E	2.41	Singlet	Solvent Impurity
F	2.16	Singlet	Methyl protons
G	1.58	Singlet	Methyl protons

Table 6. ^1H NMR data for ortho-tolunitrile.

Peak	Chemical Shift (ppm)	Multiplicity	Interpretation
A	7.68	Doublet	Nitrile phenyl proton (next to C≡N)
B	7.55	Doublet	Nitrile phenyl proton (next to CH_3)
C	7.31	Triplet	Nitrile phenyl proton
D	2.60	Singlet	Methyl protons
E	1.72	Singlet	Solvent Impurity

The NMR spectrum for ortho tolunitrile had three peaks in the 7.3-7.7 ppm range that accounted for the protons on the phenyl ring and two peaks in the 1.7-2.7 ppm range that covered the methyl group. There was an impurity peak at 1.72 ppm that came from H_2O that was a part of the NMR solvent. The C≡N group was electron deficient and withdrew electron density from the aromatic ring. The proton directly adjacent to the C≡N functional group was the most deshielded (7.68 ppm). This appeared as a doublet. The proton that was para to the C≡N group was the next most deshielded with a chemical shift of 7.55 ppm. The proton next to the methyl group

was the least deshielded with a chemical shift of 7.31 ppm. This peak was expected to be a doublet but showed up as a triplet. This is because of the overlap of peaks. There should be a total of four chemically unique phenyl hydrogens on ortho-tolunitrile, but only three peaks in that region were on the spectrum. The methyl group peak showed up as a singlet at 2.60 ppm.

The spectrum for $[Rh_2(N\{C_6H_5\}COCH_3)_4]\cdot$ortho-tolunitrile showed four distinguishable peaks for the phenyl protons. There should have been seven distinct peaks for all the chemically different protons, but they overlapped because they have such similar chemical shifts. The peaks A and B at 7.48 and 7.27 ppm represent the N-phenyl protons on the bridging ligands. These protons are the most deshielded because of the electron withdrawing property of the N—C—O functional group. The peaks C and D at 7.19 and 6.97 ppm represent the phenyl protons of the nitrile. The nitrile bound to the rhodium atom causes electron donating properties, so these were more shielded. Peak G was for the methyl group attached to ortho-tolunitrile, and peak F was for the methyl group on the bridging ligands. The methyl group that was a part of ortho-tolunitrile was more shielded than the bridging methyl group. The intensity of peak F is much higher than peak G because there are four bridging ligands for every two attached nitriles.

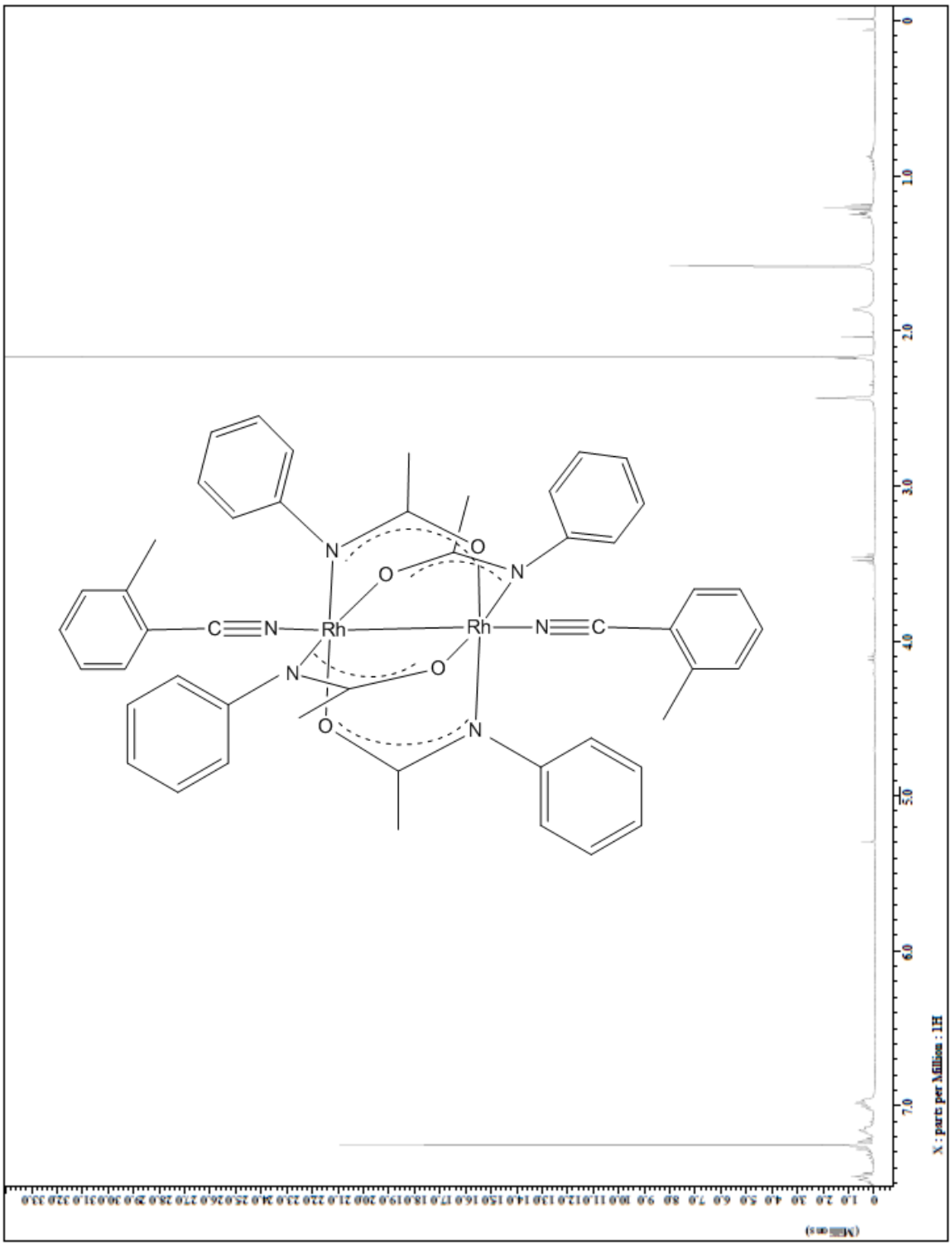

Figure 9. NMR Spectrum of 2,2-*cis* $[Rh_2(N\{C_6H_5\}COCH_3)_4]\bullet 2NC\{2\text{-}CH_3\}C_6H_4$.

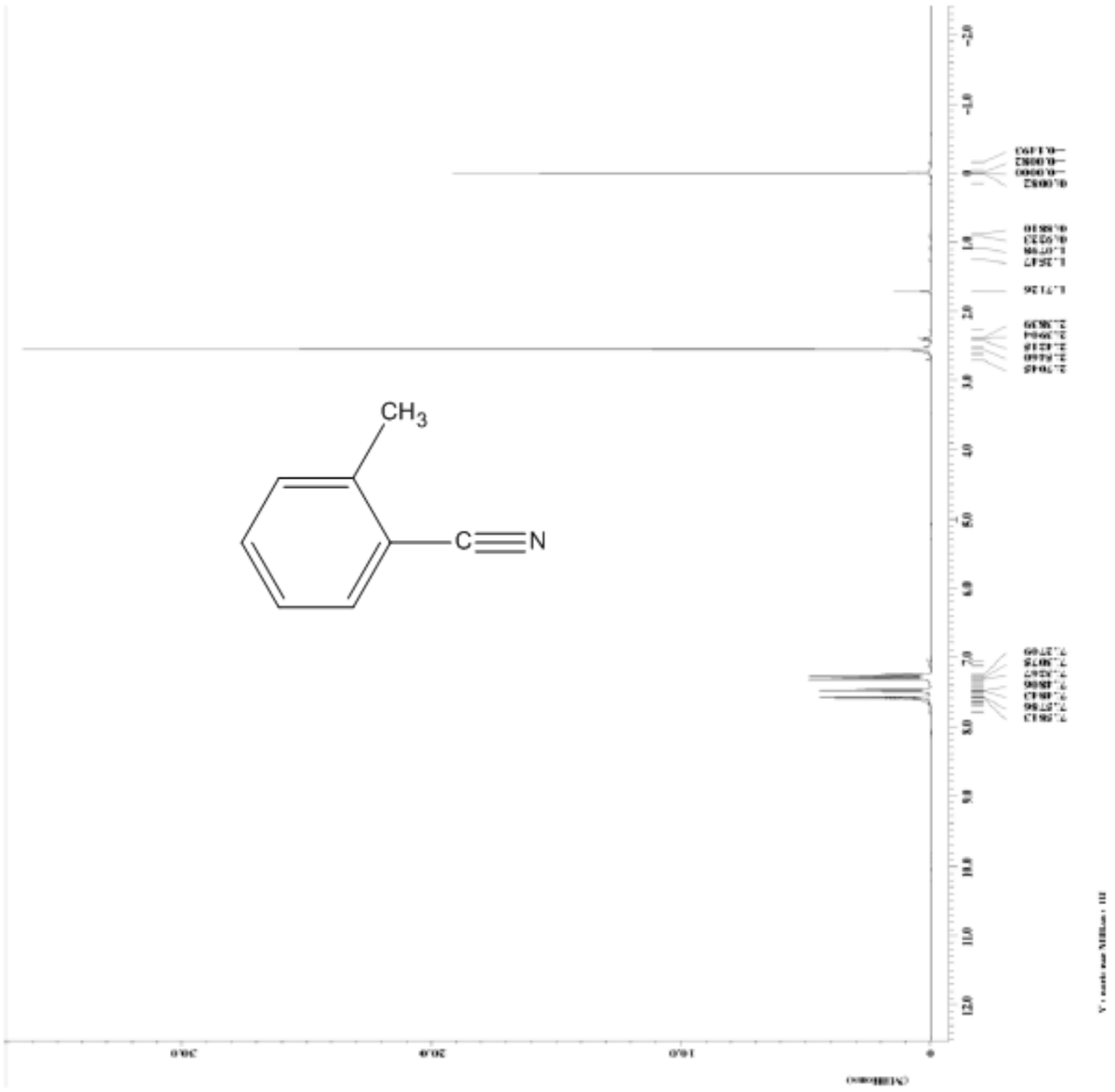

Figure 10. NMR Spectrum of NC{2-CH_3}C_6H_4.

The proton NMR spectrum for $[Rh_2(N\{C_6H_5\}COCH_3)_4]$·meta-tolunitrile is shown in Figure 11. The NMR spectrum for meta-tolunitrile isolated is shown in Figure 12. The data for peaks of interest for both of these compounds are found in Table 7 and Table 8 below.

Table 7. ^1H NMR data for $[Rh_2(N\{C_6H_5\}COCH_3)_4]$·meta-tolunitrile.

Peak	Chemical Shift (ppm)	Multiplicity	Interpretation
A	7.47	Doublet	N-phenyl protons
B	7.40	Triplet	N-phenyl protons
C	7.35	Triplet	N-phenyl protons
D	7.13	Triplet	Nitrile phenyl protons
E	7.02	Doublet	Nitrile phenyl protons
F	6.96	Doublet	Nitrile phenyl protons
G	2.39	Singlet	Methyl protons
H	2.17	Singlet	Methyl protons
I	1.59	Singlet	Solvent Impurity

Table 8. ^1H NMR data for meta-tolunitrile.

Peak	Chemical Shift (ppm)	Multiplicity	Interpretation
A	7.50	Doublet	Nitrile phenyl protons
B	7.46	Triplet	Nitrile phenyl protons
C	7.38	Doublet	Nitrile phenyl protons
D	7.30	Singlet	Nitrile phenyl protons
E	2.41	Singlet	Methyl protons
F	1.79	Singlet	Solvent Impurity

The compound meta-tolunitrile had four phenyl proton peaks in the region 7.3-7.5 ppm, and one methyl proton peak at 2.41 ppm. There was one impurity at 1.79 ppm that was accounted for by H_2O in the $CDCl_3$. The proton adjacent to the C≡N functional group was the most deshielded, and is represented by peak A. This peak was a doublet because of the one neighboring proton. The proton next to the methyl group and the C≡N group is represented by peak D, and it was a singlet.

The NMR spectrum for $[Rh_2(N\{C_6H_5\}COCH_3)_4]$·meta-tolunitrile had six phenyl proton peaks. Seven peaks were expected, but all the peaks were so close to one another it was hard to

distinguish them all. The $CDCl_3$ solvent peak that was around 7.26 ppm overlapped with the phenyl peaks, making it look distorted. The N-phenyl protons were the most deshielded, and the peaks were the farthest to the right in the spectrum. These were represented by peaks A, B, and C. The nitrile phenyl protons were more shielded because of the electron rich rhodium bound nitrile. These were represented by peaks D, E, and F. Peak G represented the methyl group protons from the bridging ligands, and peak H represented the methyl group protons from meta-tolunitrile. There was a solvent impurity shown by peak I. This was most likely due to H_2O solvent in $CDCl_3$.

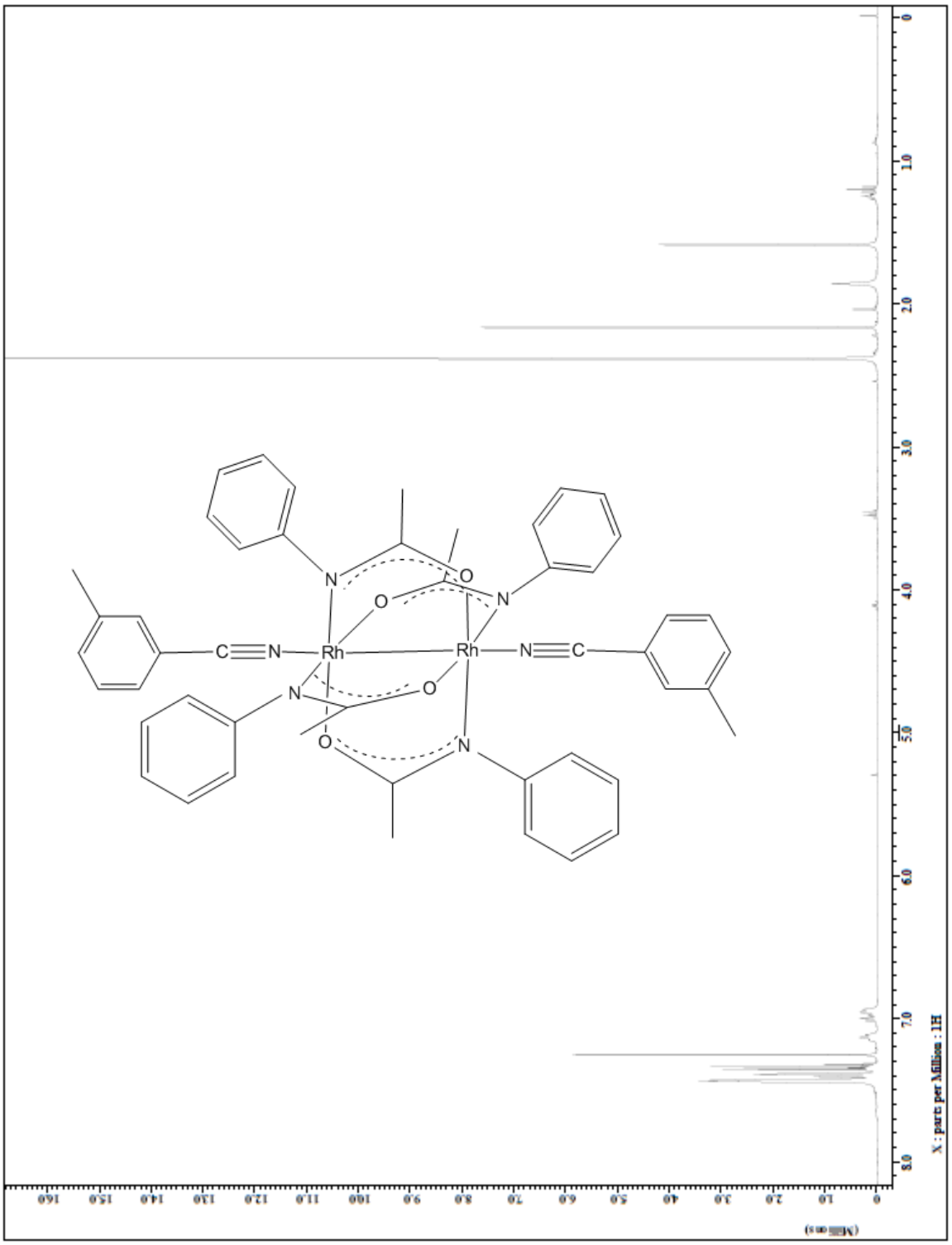

Figure 11. NMR Spectrum of 2,2-*cis* $[Rh_2(N\{C_6H_5\}COCH_3)_4]\bullet 2NC\{3\text{-}CH_3\}C_6H_4$.

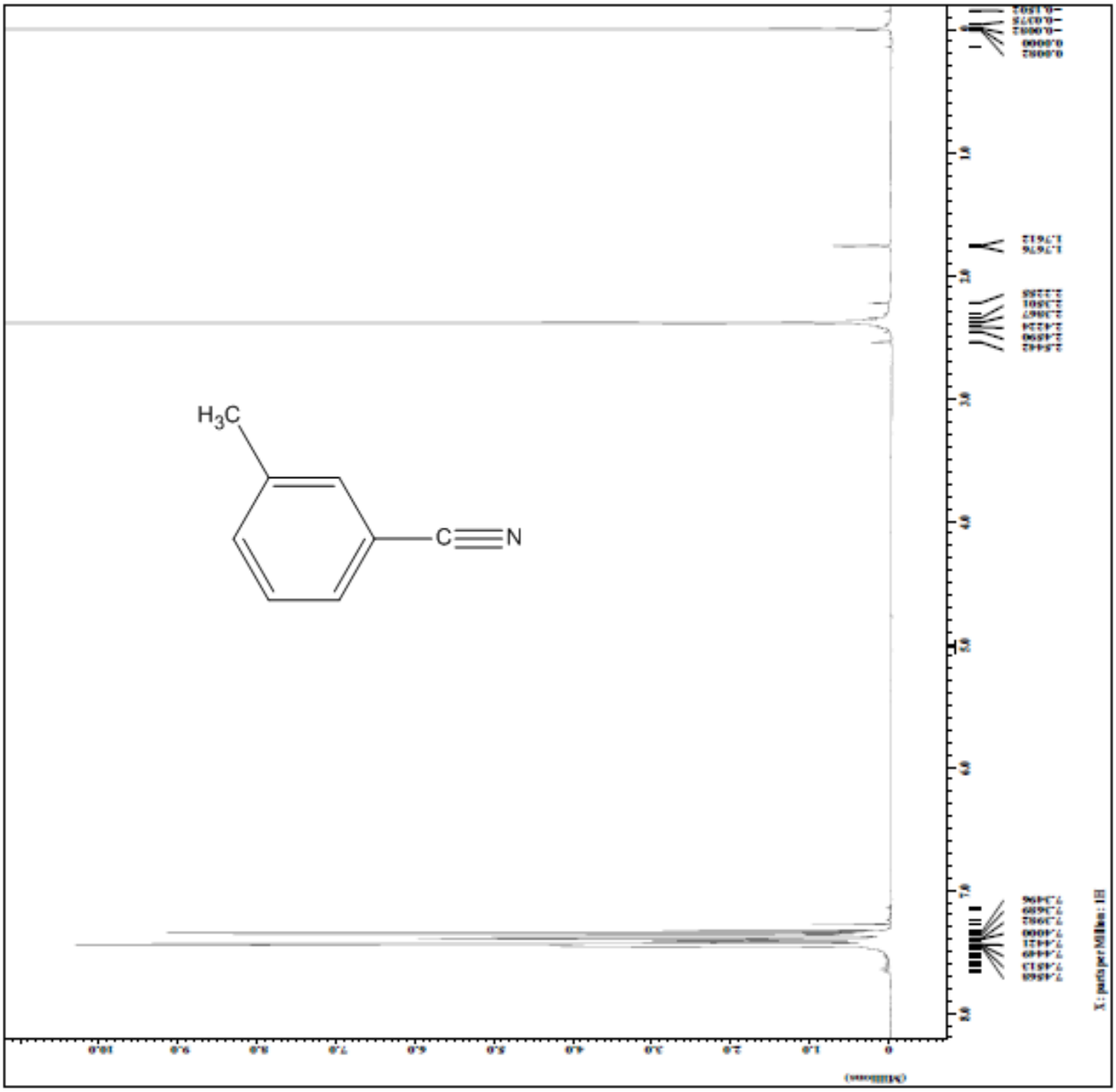

Figure 12. NMR Spectrum of NC{3-CH_3}C_6H_4.

2. FTIR Data

The FTIR (Fourier Transform Infrared Spectrometer) used was a Shimadzu IR Prestige-21. The IR spectrum was collected on each of the following molecules: 2,2-*cis* $[Rh_2(N\{C_6H_5\}COCH_3)_4]$•benzonitrile, 2,2-*cis* $[Rh_2(N\{C_6H_5\}COCH_3)_4]$•ortho-tolunitrile, 2,2-*cis* $[Rh_2(N\{C_6H_5\}COCH_3)_4]$•meta-tolunitrile, and each of the nitriles isolated. The C≡N stretching frequency of the nitrile indicates the type of bonding involved when it is bound to the Rh atom as discussed in methods and materials. σ-bonding is predominant when the stretching frequency increases because the bond is stronger and higher in energy. π-backbonding is predominant when the stretching frequency decreases because the bond is weaker and lower in energy. The C≡N stretching frequency is compared for the isolated nitrile and the bound nitrile to determine whether σ or π-backbonding is predominant.

The benzonitrile IR spectrum is shown in Figure 13. The C≡N stretching frequency was 2228.2 cm^{-1}. This nitrile C≡N stretch is consistent with the literature value of 2213 cm^{-1}. The IR spectrum of 2,2-*cis* $[Rh_2(N\{C_6H_5\}COCH_3)_4]$•$2NCC_6H_5$ is shown in Figure 14. The C≡N stretching frequency was 2358.94 cm^{-1}. When the nitrile was bound to the Rh atom, the frequency was higher in energy so σ-bonding is evident.

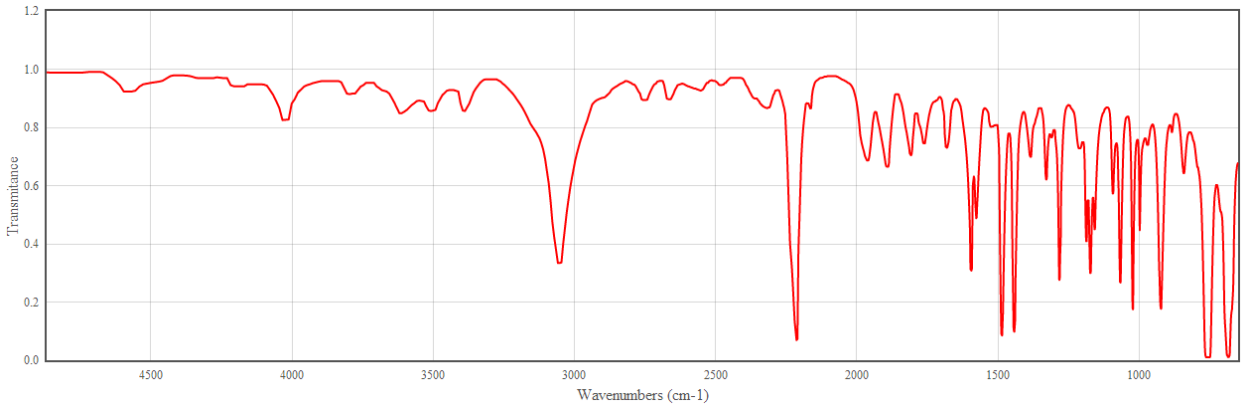

Figure 13. IR spectrum of benzonitrile.[24]

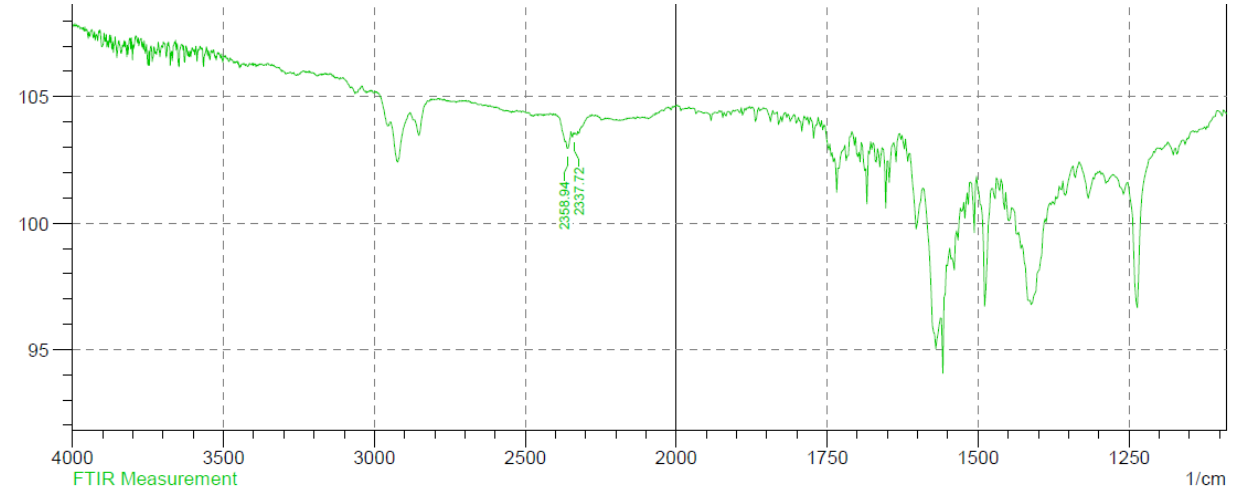

No.	Peak	Intensity	Corr. Intensity	Base (H)	Base (L)	Area	Corr. Area
1	2337.72	103.53	0.04	2339.65	2333.87	-0.09	0
2	2358.94	102.96	0.44	2366.66	2349.3	-0.23	0.02

Figure 14. IR Spectrum of 2,2-*cis* $[Rh_2(N\{C_6H_5\}COCH_3)_4]\bullet 2NCC_6H_5$.

The ortho-tolunitrile IR spectrum is shown in Figure 15. The C≡N stretching frequency was 2223.92 cm^{-1}. The IR spectrum of 2,2-*cis* $[Rh_2(N\{C_6H_5\}COCH_3)_4]\bullet 2NC\{2\text{-}CH_3\}C_6H_4$ is shown in Figure 16. The C≡N stretching frequency was 2320.37 cm^{-1}. The stretching frequency increased when ortho-tolunitrile was bound to the Rh atom similarly to benzonitrile, so σ-bonding was predominant.

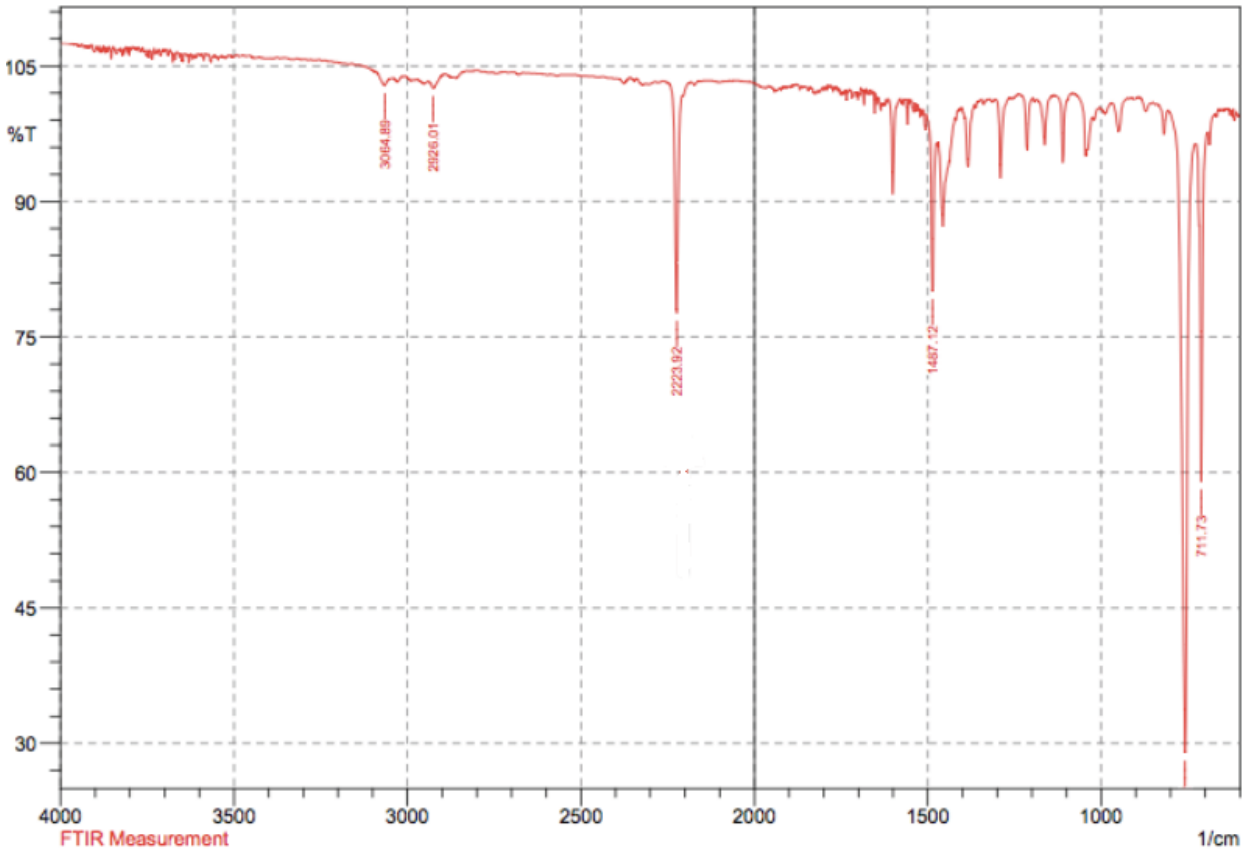

Figure 15. IR spectrum of ortho-tolunitrile.

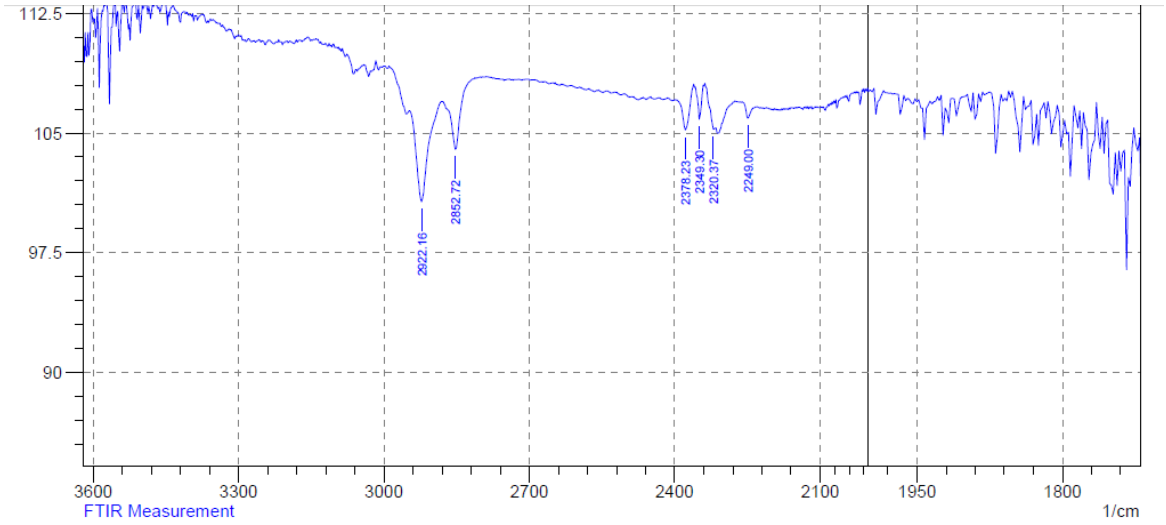

	Peak	Intensity	Corr. Intensity	Base (H)	Base (L)	Area	Corr. Area
1	2249	105.93	0.85	2260.57	2237.43	-0.63	0.03
2	2320.37	105.25	0.76	2337.72	2314.58	-0.62	0.03
3	2349.3	105.86	2.08	2357.01	2341.58	-0.45	0.07
4	2378.23	105.2	2.37	2395.59	2360.87	-0.94	0.16
5	2852.72	103.98	3.63	2881.65	2812.21	-1.95	0.3
6	2922.16	100.69	5.94	2947.23	2881.65	-1.2	0.65

Figure 16. IR Spectrum of 2,2-*cis* $[Rh_2(N\{C_6H_5\}COCH_3)_4]$•ortho-tolunitrile.

The meta-tolunitrile IR spectrum is shown in Figure 17. The C≡N stretching frequency was 2227.78 cm^{-1}. The IR spectrum of 2,2-*cis* $[Rh_2(N\{C_6H_5\}COCH_3)_4]$•$2NC\{3\text{-}CH_3\}C_6H_4$ is shown in Figure 18. The C≡N stretching frequency was 2360.87 cm^{-1}. The increase in stretching frequency from the uncomplexed meta-tolunitrile to the complexed meta-tolunitrile indicated that σ-bonding was predominant.

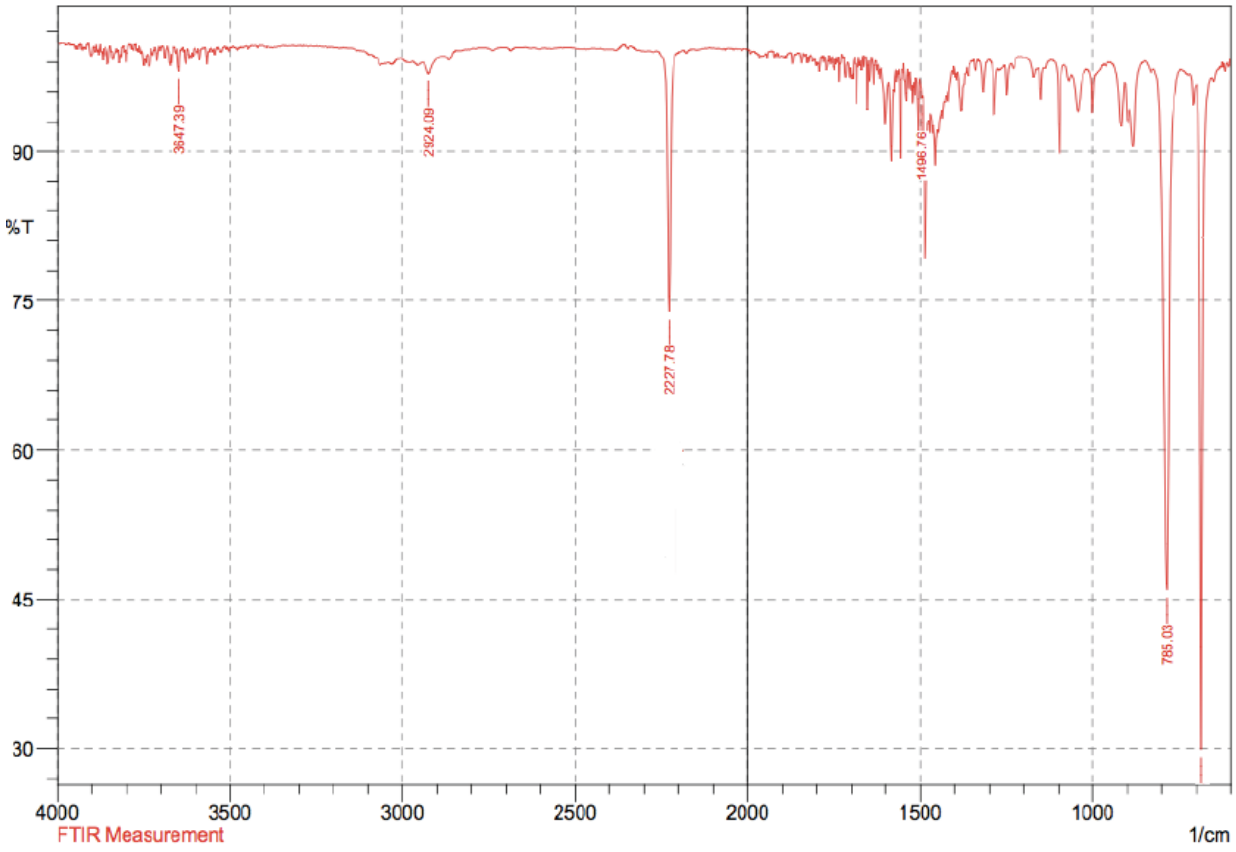

Figure 17. IR spectrum of meta-tolunitrile.

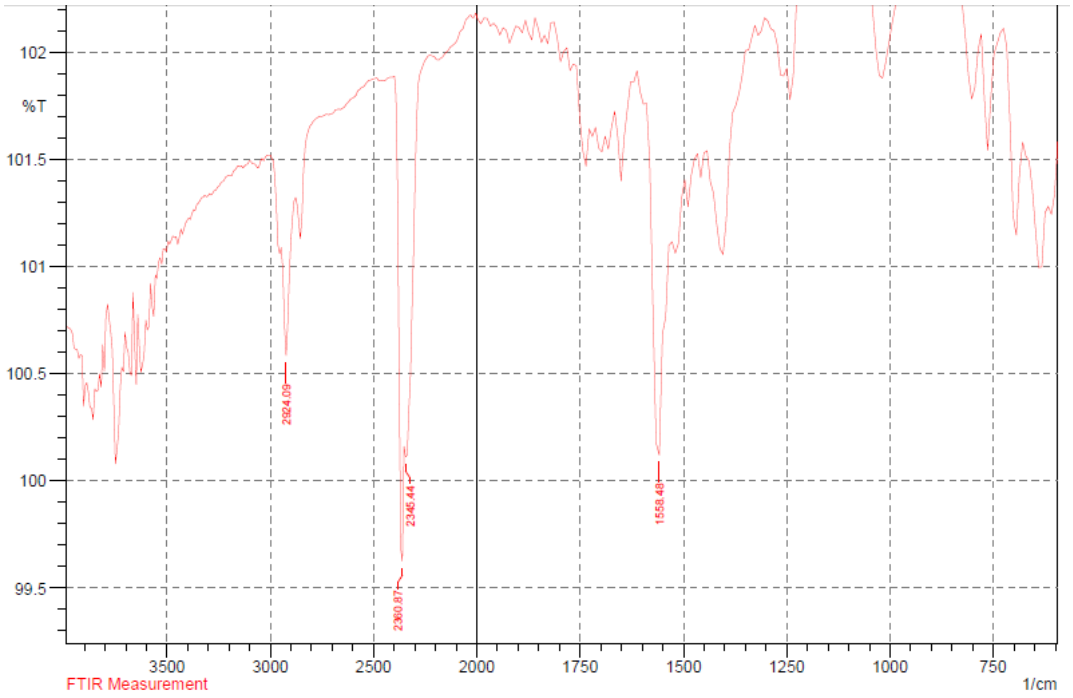

	Peak	Intensity	Corr. Intensity	Base (H)	Base (L)	Area	Corr. Area
1	1558.48	100.1215	1.3189	1589.34	1527.62	-0.2194	0.1638
2	2345.44	100.1129	0.1632	2353.16	2229.71	-0.6851	-0.1139
3	2360.87	99.6251	0.825	2399.45	2353.16	-0.1307	0.0738
4	2924.09	100.5866	0.581	2947.23	2877.79	-0.2941	0.0676

Figure 18. IR Spectrum of 2,2-*cis* $[Rh_2(N\{C_6H_5\}COCH_3)_4]$•meta-tolunitrile.

3. X-ray Diffraction Data

3.1 Crystal Growth

Benzonitrile adduct of 2,2-*cis* $[Rh_2(N\{C_6H_5\}COCH_3)_4]$

The successful structure was solved on a crystal that grew from acetone. It was a red crystal in the shape of a prism with smooth edges. The dimensions of this crystal were 0.097 x 0.244 x 0.057 mm. When acetone was used as the solvent for vapor diffusion, many red, X-ray quality crystals grew. Some other solvents grew crystals but none that would diffract properly. Hexane grew very tiny blue and red crystals. H_2O grew many large red crystals, but they were very thin and weak.

Ortho-tolunitrile adduct of 2,2-*cis* $[Rh_2(N\{C_6H_5\}COCH_3)_4]$

The successful structure was solved using a crystal that grew from methanol. This crystal was red and classified as a chunk. The dimensions of this crystal were 0.300 x 0.240 x 0.160 mm. 200 equivalents of ortho-tolunitrile were needed for coordination of the nitrile to both axial sites of the dirhodium core. An abundance of X-ray quality crystals were found in methanol. H_2O also grew crystals that appeared to be X-ray quality, but they did not show clear spots when diffracted upon. Ethyl acetate and acetone were unsuccessful solvents for crystal growth for 2,2-*cis* $[Rh_2(N\{C_6H_5\}COCH_3)_4]\bullet 2NC\{2\text{-}CH_3\}C_6H_4$.

Meta-tolunitrile adduct of 2,2-*cis* $[Rh_2(N\{C_6H_5\}COCH_3)_4]$

The meta-tolunitrile crystals were harder to grow than the ortho-tolunitrile crystals. With about the same amount of nitrile, the nitrile only coordinated to one rhodium atom. The successful structure was solved using a crystal that grew from methanol, which is the same

solvent used for the ortho-tolunitrile adduct shown above. The crystal was a red chunk. The crystal was cut to reduce the size, and doing this made the smooth edges slightly uneven. The dimensions of this crystal were 0.370 x 0.360 x 0.200 mm. 2,2-*cis* $[Rh_2(N\{C_6H_5\}COCH_3)_4]\bullet 2NC\{3\text{-}CH_3\}C_6H_5$ crystals were found in many solvents. Methanol and H_2O seemed to be the only solvents that grew X-ray quality crystals. H_2O grew crystals that were extremely tiny and thin. Methanol had a few good, thick crystals that diffracted well.

3.2 Crystallographic Data

Tables 9-11 below contain crystallographic data for each of the complexes.

Table 9. Crystallographic data for 2,2-*cis* $[Rh_2(N\{C_6H_5\}COCH_3)_4]\bullet 2NCC_6H_5$.

2,2-*cis* $[Rh_2(N\{C_6H_5\}COCH_3)_4]\bullet 2NCC_6H_5$	
Crystal Dimensions	0.097 x 0.244 x 0.057 mm
Crystal System	Monoclinic
Space Group	$P2_1/n$
Unit Cell Parameters	a = 10.2115(7) Å
	b = 9.9667(7) Å
	c = 21.367(2) Å
	β = 100.971(7)°
	V = 2134.9(3) $Å^3$
Exposure Temperature	-50.0 °C
Exposure Rate	15.0 sec/°
R_1	0.0214
R (All reflections)	0.0250
wR_2 (All reflections)	0.0542
Goodness of Fit	1.030
Max Shift/Error	0.005

Maximum peak in Final Diff. Map	0.39 $e^-/Å^3$
Minimum peak in Final Diff. Map	-0.34 $e^-/Å^3$

A red, prism crystal of 2,2-*cis* $[Rh_2(N\{C_6H_5\}COCH_3)_4]\bullet 2NCC_6H_5$ was mounted on a mitogen loop and placed in a Rigaku XtaLab Mini diffractometer for X-ray diffraction. The diffractometer used graphite monochromated Mo-κα radiation. The distance from the crystal to the detector was 50.00 mm. An exposure rate of 15.0 sec/° allowed the diffractometer to find distinct, clear spots. Data was collected at -50.0 °C to help the crystal remain stationary on the mounting pin. A unit cell was assigned with parameters listed in Table 9. The crystal was monoclinic with a primitive lattice type with $P2_1/n$ symmetry. The Z number was 2, which indicated that there were two full molecules per unit cell. The formula weight was 948.69, and the density was calculated to be 1.476 g/cm^3.

Table 10. Crystallographic data for 2,2-*cis* $[Rh_2(N\{C_6H_5\}COCH_3)_4]\bullet 2NC\{2\text{-}CH_3\}C_6H_4$.

2,2-*cis* $[Rh_2(N\{C_6H_5\}COCH_3)_4]\bullet 2NC\{2\text{-}CH_3\}C_6H_4$	
Crystal Dimensions	0.300 x 0.240 x 0.160 mm
Crystal System	Monoclinic
Space Group	$P2_1/n$
Unit Cell Parameters	a = 10.3625(8) Å
	b = 10.0489(7) Å
	c = 21.611(2) Å
	β = 100.868(7)°
	V = 2210.0(3) $Å^3$
Exposure Temperature	-50.0 °C
Exposure Rate	15.0 sec/°
R_1	0.0322

R (All reflections)	0.0399
wR_2 (All reflections)	0.0723
Goodness of Fit	1.070
Max Shift/Error	0.003
Maximum peak in Final Diff. Map	0.54 $e^-/Å^3$
Minimum peak in Final Diff. Map	-0.47 $e^-/Å^3$

A red chunk crystal of 2,2-*cis* $[Rh_2(N\{C_6H_5\}COCH_3)_4]$•$2NC\{2\text{-}CH_3\}C_6H_4$ was mounted on a mitogen loop and placed inside a diffractometer. The Rigaku XtaLAB Mini diffractometer was used with graphite monochromated Mo-κα radiation. The crystal-to-detector distance was 50.00 mm. Data was collected at -50.0 °C. The exposure rate was 15.0 sec/°, and large crisp spots were observed after diffraction. The unit cell, which is listed in Table 10, determined the crystal system to be monoclinic with a primitive lattice type. The Z value was 2 and the formula weight was 978.76, and the density was calculated to be 1.471 g/cm^3.

Table 11. Crystallographic data for 2,2-*cis* $[Rh_2(N\{C_6H_5\}COCH_3)_4]$•$2NC\{3\text{-}CH_3\}C_6H_4$.

2,2-*cis* $[Rh_2(N\{C_6H_5\}COCH_3)_4]$•$2NC\{3\text{-}CH_3\}C_6H_4$	
Crystal Dimensions	0.370 x 0.360 x 0.200 mm
Crystal System	Triclinic
Space Group	P-1
Unit Cell Parameters	a = 10.849(3) Å
	b = 11.530(3) Å
	c = 12.259(3) Å
	α = 117.562(8)°
	β = 103.061(7)°
	γ = 101.562(7)°
	V = 1238.9(6) $Å^3$

Exposure Temperature	-100.0 °C
Exposure Rate	15.0 sec/°
R_1	0.0485
R (All reflections)	0.0501
wR_2 (All reflections)	0.1326
Goodness of Fit	1.077
Max Shift/Error	0.001
Maximum peak in Final Diff. Map	3.03 $e^-/Å^3$
Minimum peak in Final Diff. Map	-1.23 $e^-/Å^3$

A red chunk crystal of 2,2-*cis* $[Rh_2(N\{C_6H_5\}COCH_3)_4]$•$2NC\{3\text{-}CH_3\}C_6H_4$ was placed on a mitogen loop mounting pin in a Rigaku XtaLAB Mini diffractometer for X-ray diffraction. The radiation source was a graphite monochromated Mo-κα. The crystal was 50.00 mm from the detector. The data was collected at -100.0 °C in hopes of a quality data set. The exposure rate was 15.0 sec/°, and clear spots were observed. The unit cell parameters determined the crystal to be triclinic with P-1 symmetry. This is the lowest symmetry space group. The Z value was 1, the formula weight was 900.64 g/mol, and the calculated density was 1.207 g/cm^3.

3.3 Structure Solution and Refinement

Benzonitrile adduct of 2,2-*cis* $[Rh_2(N\{C_6H_5\}COCH_3)_4]$

The structure of 2,2-*cis* $[Rh_2(N(C_6H_5)COCH_3)_4]$•$2NCC_6H_5$ was solved using Crystal Structure software from Rigaku. Direct methods were used to solve the structure, specifically SIR2004 was the program used. Because of symmetry, only half of the molecule was displayed to work with. Both rhodium atoms were easy to distinguish because they are metals that weigh more in comparison to the other atoms of the molecule. The tetrakis carboxamidate core was

confirmed using the knowledge that each atom should be close to 90° from each other. Isotropic thermal parameters were used to determine if assigned atoms were correct. This was done by observing how large the thermal parameters were relative to their atomic position. These values represented the vibration of atoms in the crystal lattice. Very large thermal parameters indicate a misassigned atom. The ORTEP of this crystal structure is shown in Figure 19 below. This ORTEP shows the atomic positions with an ideal bond radius of 0.02 and ellipsoids at 30% probability. Half of the molecule had atom labels because half of the molecule was generated by symmetry.

A total of 21686 reflections were collected, and 4872 were unique. All non-hydrogen atoms were refined anisotropically. All the hydrogen atoms were generated using the riding model. The data was corrected for Lorentz and polarization effects. For refinement, least squares cycles were used. 2,2-*cis* $[Rh_2(N\{C_6H_5\}COCH_3)_4]\bullet 2NCC_6H_5$ had an R_1 value of 0.0214, an R value of 0.0250, and a wR_2 value of 0.0542. These residual values measured how well the data fits the model. Considering how small the numbers are, this data set solved very well. Also, the goodness of fit indicator was 1.030 and the max shift/error in final cycle was 0.005. These values indicated a correctly solved crystal structure of 2,2-*cis* $[Rh_2(N\{C_6H_5\}COCH_3)_4]\bullet 2NCC_6H_5$.

Ortho-tolunitrile adduct of 2,2-*cis* $[Rh_2(N\{C_6H_5\}COCH_3)_4]$

The crystal structure of 2,2-*cis* $[Rh_2(N\{C_6H_5\}COCH_3)_4]\bullet 2NC\{2\text{-}CH_3\}C_6H_4$ was also solved using Rigaku's Crystal Structure software. The SIR2004 program was used to match the crystallographic data to solved crystal structures. Similar to the benzonitrile adduct, the rhodium atoms were initially discovered because of their large weight. These were the only metal atoms

found in the complex, so they were easy to pick out. The organic atoms were figured out using knowledge about the complex such as bond angles. This was slowly accomplished using trial and error. Isotropic thermal parameters were used to confirm correct atomic positions. The ORTEP of this crystal structure is shown in Figure 20 below.

Out of 20692 total reflections collected, 5066 were unique. All the atoms, with an exception of hydrogens, were refined anisotropically. The riding model was used to generate all the hydrogen atoms. The data was corrected for Lorentz and polarization effects. After each change was made to the crystal structure, least squares cycles were used. These cycles provided numerical values of how well the crystal structure fit the data. 2,2-*cis* $[Rh_2(N\{C_6H_5\}COCH_3)_4]\bullet 2NC\{2\text{-}CH_3\}C_6H_4$ had an R_1 value of 0.0322, an R value of 0.0399, and a wR_2 value of 0.0723. These small residual values indicated a good crystal structure that was publishable. The goodness of fit was 1.070, and the maximum shift/error for the final cycle was 0.003.

Meta-tolunitrile adduct of 2,2-*cis* $[Rh_2(N\{C_6H_5\}COCH_3)_4]$

The structure solution of 2,2-*cis* $[Rh_2(N\{C_6H_5\}COCH_3)_4]\bullet 2NC\{3\text{-}CH_3\}C_6H_4$ was completed similar to 2,2-*cis* $[Rh_2(N\{C_6H_5\}COCH_3)_4]\bullet 2NC\{2\text{-}CH_3\}C_6H_4$. The positions of atoms were determined one at a time using isotropic thermal parameters along with knowledge about the molecule. The SIR2004 direct method program was used to solve the structure. There were many failed attempts at solving this crystal structure before we successfully solved it. Bad data sets produced unsolvable crystal structures. This was due to difficulties with crystal growth and not obtaining a single crystal for analysis. The ORTEP of this crystal structure is shown in Figure 21 below.

There were 5651 unique reflections out of a total of 12175 reflections. All the non-hydrogen atoms were refined anisotropically. The hydrogen atoms were placed in calculated positions using the riding model. The data were corrected for Lorentz and polarization effects. Least squares refinement was used to analyze how well the structure fit the model. The complex 2,2-*cis* $[Rh_2(N\{C_6H_5\}COCH_3)_4]\bullet 2NC\{3\text{-}CH_3\}C_6H_4$ had an R_1 value of 0.0485, an R value of 0.0501, and a wR_2 value of 0.1326. These values indicated how well the data set solved. There was a goodness of fit of 1.077, and the max shift/error in the final cycle was 0.001.

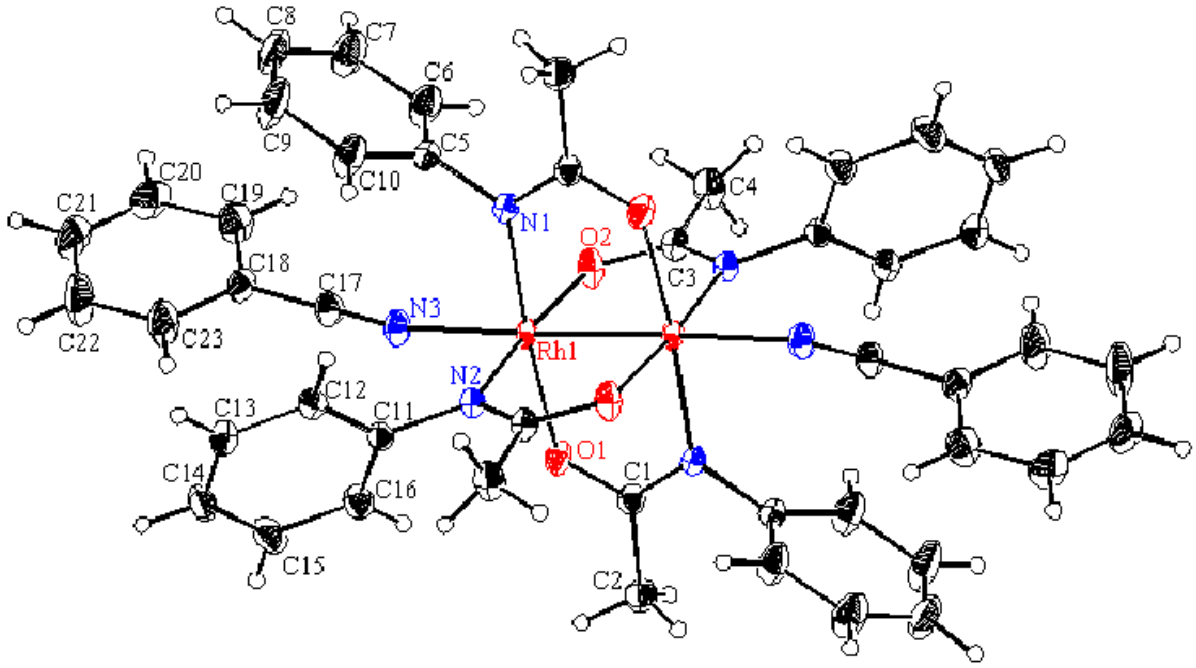

Figure 19. ORTEP of 2,2-*cis* $[Rh_2(N\{C_6H_5\}COCH_3)_4]\bullet 2NCC_6H_5$ with ellipsoids at 30% probability.

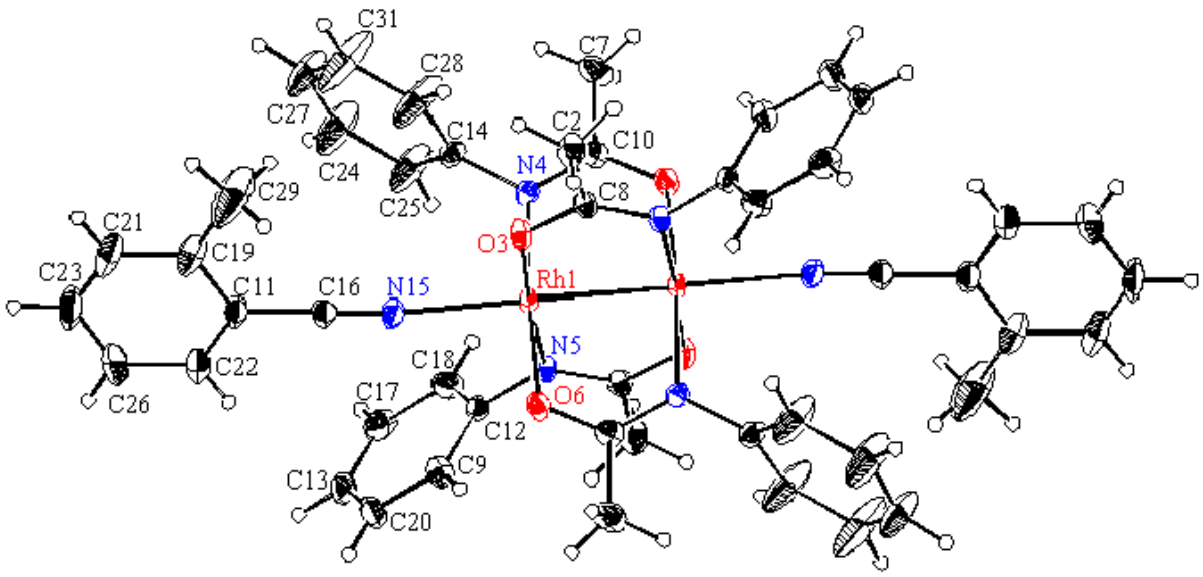

Figure 20. ORTEP of 2,2-*cis* $[Rh_2(N\{C_6H_5\}COCH_3)_4]$•$2NC\{2\text{-}CH_3\}C_6H_4$ with ellipsoids at 30% probability.

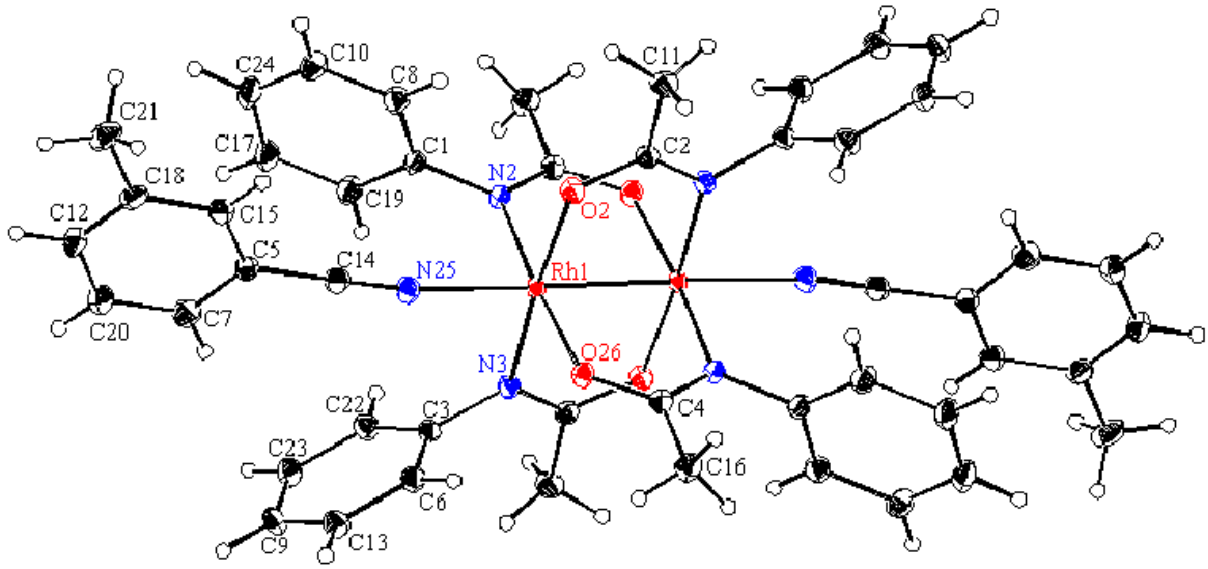

Figure 21. ORTEP of 2,2-*cis* $[Rh_2(N\{C_6H_5\}COCH_3)_4]$•$2NC\{3\text{-}CH_3\}C_6H_4$ with ellipsoids at 30% probability.

3.4 Bond Distances

Some atom abbreviations were used in the following sections. Equatorial oxygens and nitrogens are referred to as O_{eq} and N_{eq}. These are the atoms that are a part of the dirhodium phenylacetamide core. Axial nitrogens are referred to as N_{ax}. They are the atoms that are bound to the Rh—Rh bond at the catalytic site. This bond would theoretically be parallel to the rhodium Rh—Rh bond if it was perfectly linear. The 2,2-*cis* $[Rh_2(N\{C_6H_5\}COCH_3)_4]$ complex was abbreviated as Rh_2L_4 to save space in the Table.

Table 12. The bond distances of interest of 2,2-*cis* $[Rh_2(N\{C_6H_5\}COCH_3)_4]\bullet 2NCC_6H_5$, 2,2-*cis* $[Rh_2(N\{C_6H_5\}COCH_3)_4]\bullet 2NC\{2\text{-}CH_3\}C_6H_4$, and 2,2-*cis* $[Rh_2(N\{C_6H_5\}COCH_3)_4]\bullet 2NC\{3\text{-}CH_3\}C_6H_4$.

Bond Distances (Å)			
	$Rh_2L_4\bullet 2NCC_6H_5$	$Rh_2L_4\bullet 2NC\{2\text{-}CH_3\}C_6H_4$	$Rh_2L_4\bullet 2NC\{3\text{-}CH_3\}C_6H_4$
Rh—Rh	2.4319(3)	2.4342(3)	2.4249(6)
Rh—O_{eq}	2.0438(14)	2.0535(19)	2.047(4)
Rh—N_{eq}	2.0465(14)	2.049(3)	2.050(3)
Rh—N_{ax}	2.2228(16)	2.234(3)	2.217(5)
N—C	1.135(3)	1.138(4)	1.138(7)
Note that Rh_2L_4 stands for 2,2-*cis* $[Rh_2(N\{C_6H_5\}COCH_3)_4]$.			

The benzonitrile, o-tolunitrile, and m-tolunitrile adducts of 2,2-*cis* $[Rh_2(N\{C_6H_5\}COCH_3)_4]$ all had very similar bond distances. The Rh—Rh bond distance was 2.43 Å for benzonitrile, 2.43 Å for o-tolunitrile, and 2.42 Å for m-tolunitrile. This data was very similar to Bear and Kadish's published crystal structure of the 2,2-cis structure with DMSO as the axial ligands. The Rh—Rh bond length was 2.448 Å. The Rh—O_{eq} and Rh—N_{eq} bond

distances ranged between 2.04 - 2.05 Å for the benzonitrile, o-tolunitrile, and m-tolunitrile adducts. Bear and Kadish's bond distances ranged between 2.03-2.06, which is very similar. The Rh—N_{ax} bond distance for benzonitrile was 2.22 Å, o-tolunitrile was 2.23 Å, and m-tolunitrile was 2.21 Å. The axial ligand bond distance cannot be compared with Bear and Kadish's work because DMSO has completely different properties. The N—C bond distance was about 1.13 Å for each of the adducts. This short bond distance confirms the presence of the nitrile's triple bond between N_{ax} and C. Such similar bond distances for the benzonitrile, o-tolunitrile, and m-tolunitrile adducts of 2,2-*cis* $Rh_2(N(C_6H_5)COCH_3)_4$ indicates that the bond dissociation energy and bond strength did not significantly change when the different nitriles were bound to the dirhodium phenylacetamide core.

3.5 Bond Angles and Torsion Angles

The bond angles for each of the three 2,2-*cis* $[Rh_2(N\{C_6H_5\}COCH_3)_4]$ compounds gave insight into the structural properties of the molecules. The individual atoms are numbered in each of the ORTEP diagrams shown in Figures 19-21. This numbering scheme was used to explain some of the bond and torsion angles.

Table 13. Bond angles and torsion angles of interest for 2,2-*cis* $[Rh_2(N\{C_6H_5\}COCH_3)_4]\bullet 2NCC_6H_5$, 2,2-*cis* $[Rh_2(N\{C_6H_5\}COCH_3)_4]\bullet 2NC\{2\text{-}CH_3\}C_6H_4$, and 2,2-*cis* $[Rh_2(N\{C_6H_5\}COCH_3)_4]\bullet 2NC\{3\text{-}CH_3\}C_6H_4$.

Bond Angles and Torsion Angles(°)			
	$Rh_2L_4\bullet 2NCC_6H_5$	$Rh_2L_4\bullet 2NC\{2\text{-}CH_3\}C_6H_4$	$Rh_2L_4\bullet 2NC\{3\text{-}CH_3\}C_6H_4$
Rh—N_{ax}—C	167.15(15)	173.4(3)	164.5(5)
N_{eq}—Rh—Rh'—O'_{eq}	1.63(4)	2.22(6)	1.80(6)

O_{eq}—Rh—Rh'—N'_{eq}	1.78(4)	1.56(6)	1.44(11)
Note that Rh_2L_4 stands for 2,2-*cis* $[Rh_2(N\{C_6H_5\}COCH_3)_4]$.			

The bond angle between the rhodium atom, axial nitrogen, and carbon (Rh—N≡C) would be expected to be linear (180°) because of the triple bond between the N and C. Experimentally, this was not observed. The benzonitrile adduct of 2,2-*cis* $[Rh_2(N\{C_6H_5\}COCH_3)_4]$ has an angle of 167°, the o-tolunitrile adduct of 2,2-*cis* $[Rh_2(N\{C_6H_5\}COCH_3)_4]$ has an angle of 173°, and the m-tolunitrile adduct of 2,2-*cis* $[Rh_2(N\{C_6H_5\}COCH_3)_4]$ angle was 164°. The o-tolunitrile adduct had the Rh—N≡C angle that was closest to linearity. The benzonitrile adduct was expected to have the closest angle to 180° because there is less steric hindrance on the nitrile. The methyl group in the ortho position of the phenyl ring on o-tolunitrile takes up more space. It did not seem to make a difference. The m-tolunitrile adduct has the farthest angle from 180°, even though it was not that far from it. This makes sense because the methyl group was in the meta position on the phenyl ring of the nitrile.

The torsion angles, also known as dihedral angles, would be expected to be at 0°. They measure the angle between the bridging parallel carboxamidate nitrogens and oxygens. The benzonitrile adduct of 2,2-*cis* $[Rh_2(N\{C_6H_5\}COCH_3)_4]$ had torsion angles of 1.63° for N1—Rh1—Rh1'—O1' and 1.78° for N2—Rh1—Rh1'—O2'. The ortho-tolunitrile adduct of 2,2-*cis* $[Rh_2(N\{C_6H_5\}COCH_3)_4]$ had torsion angles of 2.22° for N4—Rh1—Rh1'—O6' and 1.56° for O3—Rh1—Rh1'—N5'. The meta-tolunitrile adduct of 2,2-*cis* $[Rh_2(N\{C_6H_5\}COCH_3)_4]$ had torsion angles of 1.80° for O2—Rh1—Rh1'—N3' and 1.44° for N2—Rh1—Rh1'—O26'. Each adduct had a slight twist from planarity. This is either due to steric hindrance or electronic

properties. This was unlike the 2,2-*trans* $[Rh_2(N\{C_6H_5\}COCH_3)_4]$ molecules when bound to nitriles which have larger torsion angles of about ten degrees.[11]

3.6 Packing Diagrams

The packing diagrams for 2,2-*cis* $[Rh_2(N\{C_6H_5\}COCH_3)_4] \bullet 2NCC_6H_5$, 2,2-*cis* $[Rh_2(N\{C_6H_5\}COCH_3)_4] \bullet 2NC\{2\text{-}CH_3\}C_6H_4$, and 2,2-*cis* $[Rh_2(N\{C_6H_5\}COCH_3)_4] \bullet 2NC\{3\text{-}CH_3\}C_6H_4$ are shown below in Figures 22-24. The packing diagrams showed how the molecule fit inside the three dimensional unit cell. Each of these packing diagrams are shown along the B axis. The packing forces were shown by visually observing how closely the molecules fit together.

The packing diagram of 2,2-*cis* $[Rh_2(N\{C_6H_5\}COCH_3)_4] \bullet 2NCC_6H_5$ showed half of four molecules fitting inside the unit cell. This means a total of two molecules were contained inside the unit cell. The crystal structure was not significantly affected by crystal packing forces. This was confirmed by the small torsion angles discussed earlier. The orderly arrangement of complexes shown in Figure 22 was repeated throughout the entire crystal lattice.

The packing diagram of 2,2-*cis* $[Rh_2(N\{C_6H_5\}COCH_3)_4] \bullet 2NC\{2\text{-}CH_3\}C_6H_4$ showed two molecules that fit in the unit cell. There was one entire molecule in the center of the cell and one quarter of four other molecules. This complex had a Z value of 2, which was similar to the benzonitrile adduct. The packing forces were observed visually, and they did not distort the crystal structure. This was confirmed with the small torsion angles (2.22° and 1.56°).

The packing diagram of 2,2-*cis* $[Rh_2(N\{C_6H_5\}COCH_3)_4] \bullet 2NC\{3\text{-}CH_3\}C_6H_4$ differed from the benzonitrile and ortho-tolunitrile adduct because only one molecule fit in the unit cell (Z value of 1). One quarter of four molecules were shown in the unit cell. The packing forces

did not appear to be very strong because all the functional groups fit nicely together in the packing diagram. Also, the small torsion angles confirm this.

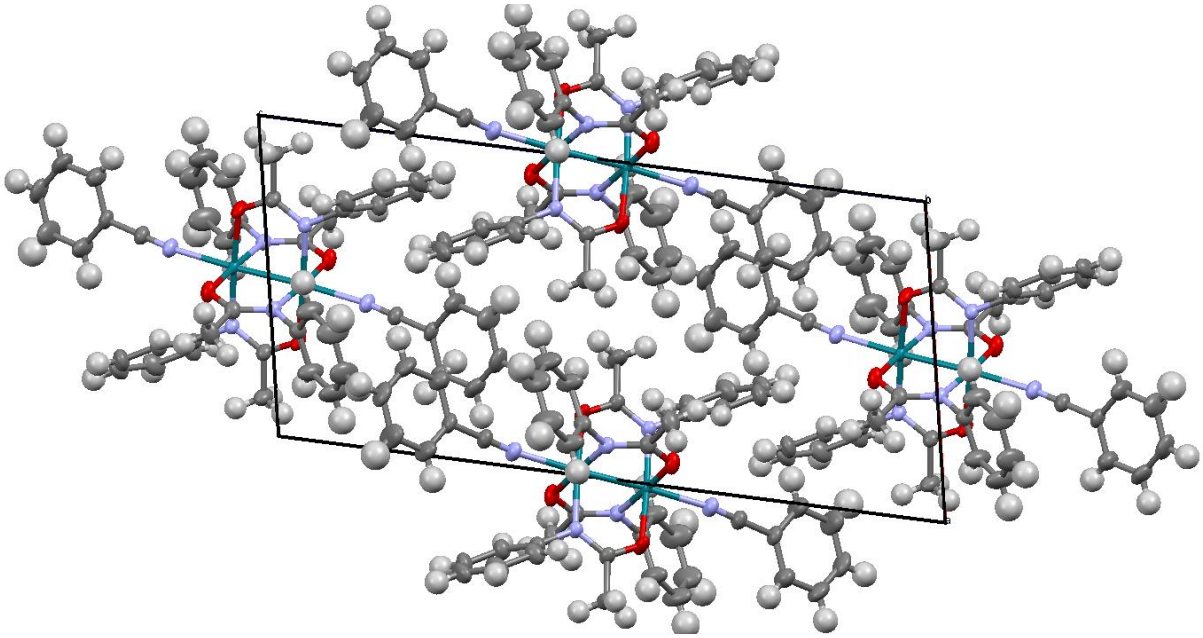

Figure 22. The packing Diagram of 2,2-*cis* $[Rh_2(N\{C_6H_5\}COCH_3)_4]\bullet 2NCC_6H_5$ looking along the B axis.

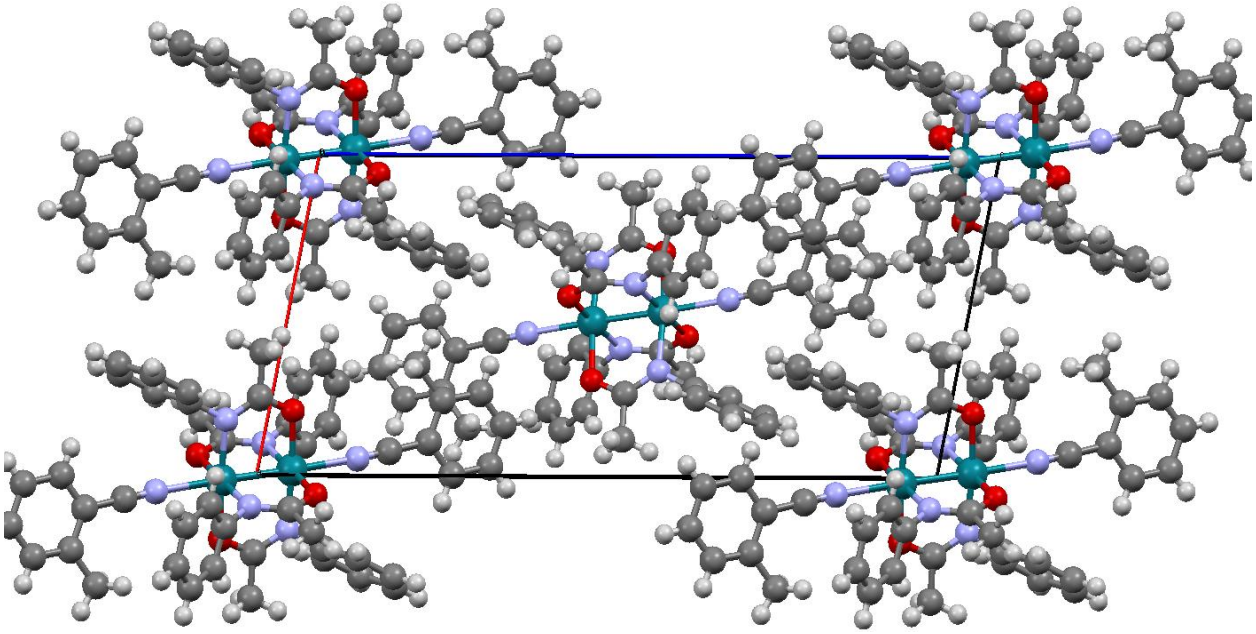

Figure 23. The packing Diagram of 2,2-*cis* $[Rh_2(N\{C_6H_5\}COCH_3)_4]\bullet 2NC\{2\text{-}CH_3\}C_6H_4$ looking along the B axis.

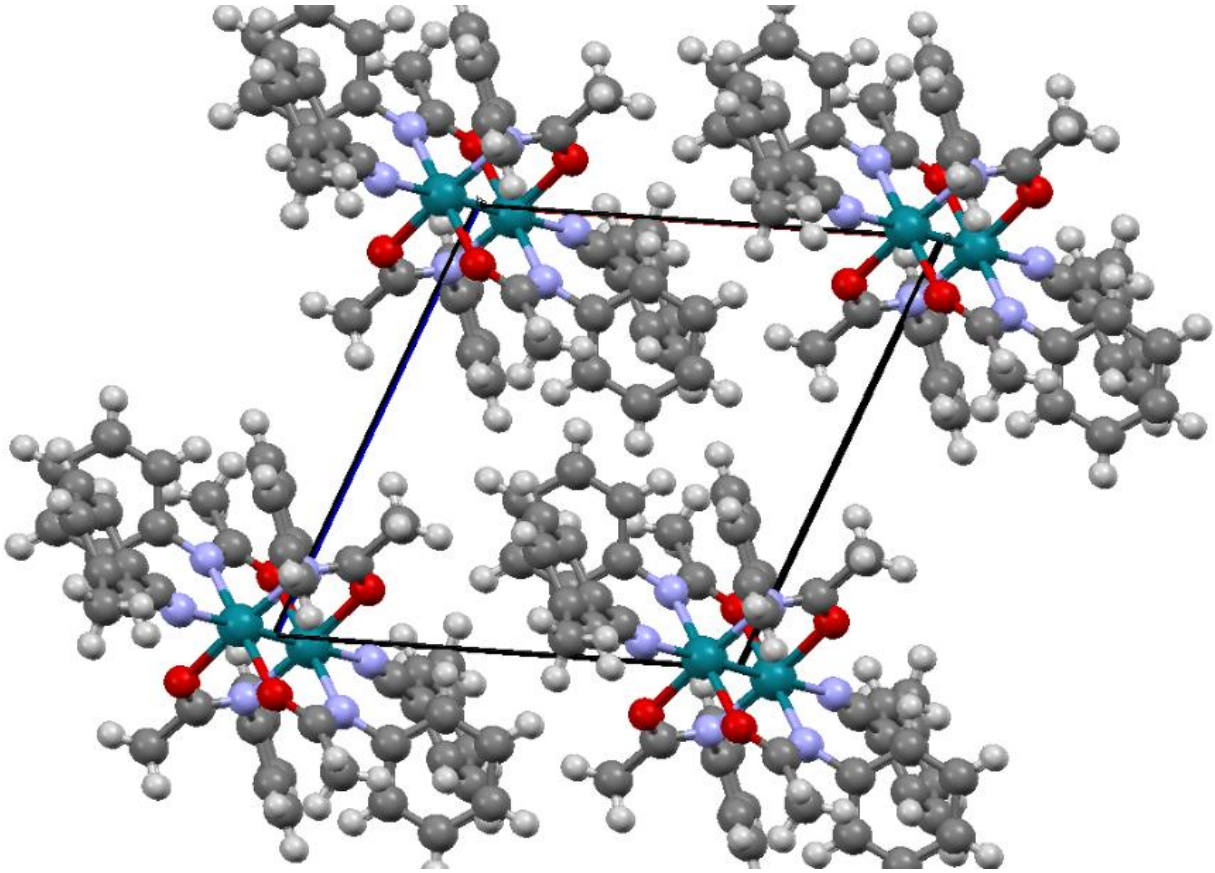

Figure 24. The packing Diagram of 2,2-*cis* $[Rh_2(N\{C_6H_5\}COCH_3)_4]\bullet 2NC\{3\text{-}CH_3\}C_6H_4$ looking along the B axis.

Conclusions

Synthesizing the benzonitrile adduct of 2,2-*cis* $[Rh_2(N\{C_6H_5\}COCH_3)_4]$ only required two equivalents of the nitrile added to the dirhodium phenylacetamide core to achieve coordination to both axial sites. Two equivalents of ortho-tolunitrile and meta-tolunitrile ligands did not successfully bind to both catalytic sites. A large excess of ortho-tolunitrile and meta-tolunitrile were required for both those adducts of 2,2-*cis* $[Rh_2(N\{C_6H_5\}COCH_3)_4]$. Two-hundred equivalents of each nitrile were added to the dirhodium phenylacetamide core to achieve coordination to both axial sites.

The bonding mode at each catalytic site of 2,2-*cis* $[Rh_2(N\{C_6H_5\}COCH_3)_4]$ was determined to be σ bonding for benzonitrile, ortho-tolunitrile, and meta-tolunitrile adducts. This was determined with FTIR by comparing the C≡N stretching frequency for each complex and the isolated nitrile. When the nitrile was bound to the dirhodium complex, there was an increase in the stretching frequency.

The crystal structures for 2,2-*cis* $[Rh_2(N\{C_6H_5\}COCH_3)_4]$•benzonitrile, 2,2-*cis* $[Rh_2(N\{C_6H_5\}COCH_3)_4]$•ortho-tolunitrile, and 2,2-*cis* $[Rh_2(N\{C_6H_5\}COCH_3)_4]$•meta-tolunitrile were consistent with literature. They all had similar bond distances and angles. The Rh—N≡C bond angle was found to not be linear due to steric hindrance of the molecule. There were small torsion angles (dihedral angles) that indicated only slight twisting. This showed that crystal packing forces did not significantly influence these molecules.

The molecules of 2,2-*cis* $[Rh_2(N\{C_6H_5\}COCH_3)_4]$•benzonitrile, 2,2-*cis* $[Rh_2(N\{C_6H_5\}COCH_3)_4]$•ortho-tolunitrile, and 2,2-*cis* $[Rh_2(N\{C_6H_5\}COCH_3)_4]$•meta-tolunitrile

had very similar properties. This indicated that varying the axially bound nitrile did not significantly change the electronic and structural characteristics of the dirhodium catalyst.

References:

[1] Parshall, G. W.; Nugent, W. A. *Chemtech.* **1988**, 18, 184.

[2] Eagle, C. T.; Farrar, D.; Holder, G. N.; et al. *Tetrahedron Letters*. 44, **2003**, 2593-2595.

[3] McLaughlin Gormley King Company. Pyrethrum: Nature's Insecticide. http://www.pyrethrum.com/FAQs.aspx (accessed October 13, 2013).

[4] National Pesticide Information Center. http://npic.orst.edu/factsheets/pyrethrins.pdf (accessed October 13, 2013).

[5]Extoxnet. Pyrethrins. http://pmep.cce.cornell.edu/profiles/extoxnet/pyrethrins-ziram/pyrethrins-ext.html (accessed October 13, 2013).

[6] Environmental Protection Agency. Lethal Dosage LD50 Values. http://www.epa.gov/oecaagct/ag101/pestlethal.html (accessed October 28, 2013).

[7] R. Paulissen, H. Reimlinger, E. Hayez, A.J. Hubert, Ph. Teyssie. *Tetrahedron Letters*. **1973**, 2233.

[8] Cotton, F. A.; Walton, R. A. Multiple Bonds Between Metal Atoms; Wiley: New York, **1982**.

[9] Johnson, S. A.; Hunt, H. R.; Neumann, H. M. *Inorg. Chem*. **1963**, 2, 960-962.

[10] Bear, J. L.; Kadish, K. M; et al. *Inorg. Chem*. **1987**, 26, 830-836.

[11] Eagle, C. T.; Farrar, D.; Holder, G. N.; Pennington, W. T.; Bailey, R. D. *J. Organomet. Chem*. 596, **2000**, 90-94.

[12] Eagle, C. T.; Kpogo, K. K.; Zink, L. C.; Smith, A. E. *Acta. Cryst.* **2012**, E68, m877.

[13] Doyle, M. P.; Griffin, J. H.; Bagheri, V.; Dorow, R. L. *Organomet*. **1984**, 3, 53-61.

[14] Doyle, M. P.; Bagheri, V.; Wandless, T. J.; Harn, N. K.; Brinker, D. A.; Eagle, C. T.; Loh, K. *J. Am. Chem. Soc.* **1990**, 112, 1906.

[15] Doyle, M. P.; Loh, K.; DeVries, K. M.; Chinn, M. S. *Tetrahedron Letters*. **1987**, 28, 8, 833-836.

[16] Drago, R. S.; Long, J. R.; Cosmano, R. *Inorg. Chem*., **1982**, 21, 2196-2202.

[17] Toreki, R. Alkyne Complexes. http://www.ilpi.com/organomet/alkyne.html (accessed September 28, 2013).

[18]Miessler, G. L.; Tarr, D. A. Inorganic Chemistry. Prentice Hall: New York, **2010**.

[19] Chemical Bonding. http://hyperphysics.phy-astr.gsu.edu/hbase/chemical/bond.html (accessed September 24, 2013).

[20] Carleton College. Single Crystal X-ray Diffraction. http://serc.carleton.edu/research_education/geochemsheets/techniques/SXD.html (accessed September 24, 2013).

[21] Nelson, S. A. X-ray Crystallography. http://www.tulane.edu/~sanelson/eens211/x-ray.htm (accessed July 17, 2013).

[22] X-ray Diffraction. http://web.pdx.edu/~pmoeck/phy381/Topic5a-XRD.pdf (accessed October 1, 2013).

[23] Eagle, C. T.; Farrar, D.; Holder, G. N.; Hatley, M. L.; Humphrey, S. L.; Olson, E. V.; Quintos, M.; Sadighi, J.; Wideman, T. *Tetrahedron Letters*. 44, **2003**, 2593-2595.

[24] National Institute of Standards and Technology. Benzonitrile. http://webbook.nist.gov/cgi/cbook.cgi?ID=C100470&Type=IR-SPEC&Index=1#IR-SPEC (accessed November 1, 2013).